POLITECNICO DI MILANO

School of Industrial and Information Engineering

Master of Science in Mechanical Engineering

Elder people fall: experimental studies with a crash test dummy

Supervisor: Ing. Marco TARABINI

Authors:
Resul Ilhan 814398
Yasin Balcik 814358

Academic Year 2014 – 2015

Table of Contents

Table List

Figure List

Abstract

Falls have always been a frequent and complex problem that might cause fatality, morbidity, loss or damage of body functions and undesired health care needs. Senior citizens are fatally affected from falls; in this thesis, the falling kinematics are analysed by means of 3-axial accelerometers placed on head and torso of a crush test dummy that we used for fall simulations. This configuration reflects the situation in which the subjects do not have any voluntary reaction to possible injuries, which is similar to what occurs during elders' fall. Accelerations were measured upon varying the dummy posture; data obtained from accelerometers were compared with data obtained with a vision system based on a commercial camera. The comparison was based on both the peak velocity and on the fall duration. With the vision system, the velocity was identified by deriving the trajectories of specific body segments using a manual video processing logic implemented in MATLAB. Data showed the compatibility between the data measured with the two different methods, outlining the possibility of identifying the peak velocity from videos available on the internet captured, for instance by video surveillance cameras.

Keywords: fall, dummy, elder people, measurement, accelerometer, video processing

Sommario

Le cadute sono un problema complesso e frequente che possono causare infortuni anche gravi. Gli anziani sono spesso soggetti a cadute e diversi studi si sono focalizzati sulla modalità di identificazione della caduta tramite segnali accelerometrici misurati da dispositivi indossabili. I livelli di soglia vengono identificati analizzando le cadute di atleti o di persone sane, con evidenti limiti dovuti alla struttura muscolare e ai riflessi differenti. Il presente lavoro si propone e di analizzare la caduta di una persona non cosciente, rappresentata nel nostro caso da un manichino da crash test strumentato mediante accelerometri. Le accelerazioni del manichino sono state misurate alla testa, nel busto e all'addome. In parallelo sono stati acquisiti i filmati della caduta, che sono stati poi analizzati tramite logiche opportunamente implementate in MATLAB. Le accelerazioni di picco e la durata della caduta sono stati studiati al variare del tipo di caduta (avanti, indietro o laterale, da seduto o in piedi, con o senza ostacoli). La cinematica della caduta identificata tramite accelerometri è stata confrontata con quella misurata dal sistema di visione. La compatibilità tra risultati apre la strada allo studio della cinematica della cadute tramite sistemi di videosorveglianza, come illustrato in due casi studio presentati nel presente lavoro.

Parole chiave: caduta, anziani, manichini, misure, manichino, analisi immagini.

1. Introduction

1.1 Introduction

A fall is the phenomenon that ends up with a person coming to rest unexpectedly on the floor. Falls are the frequent and complex problems that might cause fatality, morbidity, loss or damage of functions and undesired health care needs [1]. Each year approximately 424.000 individuals die due to falls and fatally effected people are especially adults older than 65 [2].

Several studies focused on understanding the effects of the falls on the people, factors effecting dangerousness of the falls and reducing the time for incident detection. In general, three approaches are used in order to analyse or detect the fall [3]. First approach is implemented by usage of wearable or mountable (in case of dummy analysis) sensors. The acceleration of specific body segments provides a basis to investigate or detect the fall. The second group of approaches is ambient device based approach. This approach attempts to obtain information about the fall by audio signals or by sensing the vibration on the floor on which the subjects fall. Third approach is camera-based approach. In this category, the videos have been used for the detection of the fall, but to date has never been used to identify the peak accelerations deriving from the fall. Cameras ability to detect the multiple dynamic events concurrently with less intrusion is exploited in this approach [4]

The literature focused on the fall detection is definitely broad. Jia et al. stated that technologic improvement in micro electro-mechanical system (MEMS) acceleration sensors made possible to detect the falls by means of three axis integrated MEMS accelerometers with the technique based on detection of motion and body position of an individual, wearing a sensor, by considering acceleration changes in three axes [5].

A.K. Bourke, J. O'Brien and G.M. Lyons studied detection of the fall by using single threshold determined from fall-event data set, which is created from the data obtained from tri-axial accelerometer sensors located on the trunk. The data set is composed by falls of young and healthy subjects and by the daily living activities of elder subjects [6].

Fanta, Kubový, Lopot, Pánková and Jelen worked on the kinematic analysis of backward falls of subject and dummy in relation to head injury. Calculation of the head injury criteria is carried out by using measured head acceleration hence the relation of head injury severity and kinematics of the fall is investigated [7]. The work of Fanta et

al. is important, given that it points out the reliability of data measured on the crash test dummy and can be considered as a basis for our study; unfortunately, the study does not include the falls from the sitting posture or the falls against objects, that are compulsory for a complete description of elder fall in domestic environment.

The acceleration-time history obviously allows obtaining other kinematic information as velocity or displacement, often used to make inference about the falling mechanics. In addition, using recorded video of the falls provides visibility advantage for the analysis and by video processing, it is possible to define trajectories of body parts as well as finding displacement, velocity and acceleration values of them by appropriate logics created on used software.

1.2 Proposed Method

Factors that may affect the kinematics of subjects' fall are:

- Arm arrest type
- Distance between feet
- Fall height
- Fall trajectory
- Pre-fall condition

To understand the effects of these influencing factors on people's fall we have analysed two indexes, i.e. the peak acceleration and the fall duration. Results are then compared with those obtained by a video processing performed in MATLAB; the correlation between velocities obtained from video and accelerations obtained from body-attached accelerometers. The approach is shown in Figure 1:

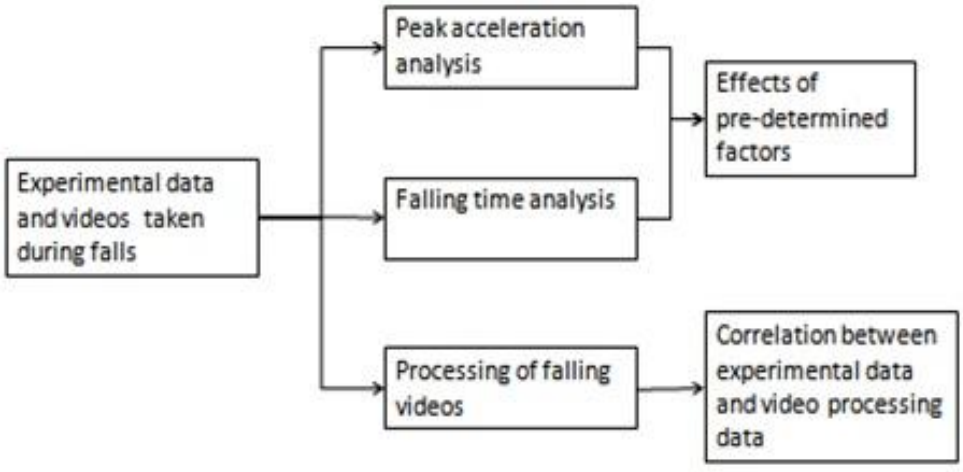

Figure 1 *Approach followed for the project*

Peak acceleration and falling time analysis are based on the detection of accelerations obtained from two 3-axial and one mono-axial accelerometer attached on a crash-test dummy. 3-axial accelerometers are placed in the head and on the torso while mono-axial accelerometer is placed on the abdomen. A movie of each fall was taken from the side of the dummy with a camera equipped with a wide-angle lens. Images were afterwards processed with MATLAB to obtain the velocities of each part we focused on; velocities are eventually compared with accelerometer data.

The peak accelerations and the durations of the falls were analysed upon varying the fall parameters and the effect of influencing factors was studied with boxplots. The magnitude of the peak acceleration was also studied in order to assess the severity of the fall.

1.3 Scheme of the thesis

The detailed description of the methods is presented in Chapter 2, which describes the procedures used for peak acceleration analysis, falling times analysis and video processing. Experimental results are presented in Chapter 3. Chapter 4 includes the discussion of the results and the conclusions are drawn in Chapter 5.

2 Method

2.1 Experiment

The elder falls shows different characteristics compared to healthy subject's falls, mainly because the elder people's striated muscles shows degeneration and loss of strength due to advanced age [8]. Elder's falls often happens near a bed or chair due to loss of conciseness results from decreasing blood pressure [9]. To date, the majority of studies aiming to assess the acceleration peaks due to falls is performed on healthy young athletes (for obvious safety reasons). Elder subjects rarely manage to arrest themselves with arms before falling; consequently are exposed to different accelerations with respect to the young subjects. All these reasons lead us to use a dummy for understanding the acceleration experienced without any conscious action from the operator. Tests were performed with a Humanetics pedestrian crash test dummy. Accelerations were measured on the dummy frame, in order to simulate the vibration level occurring at the bones.

2.1.1 Experimental Setup

Humanetics is the global pioneer in the design, development and production of anthropomorphic test devices (ATDs). They have wide range of products in various sizes including regulated and non-regulated ATDs. The products are generally used in automotive, military and aerospace industries. Crash Test Dummy is used for simulation of human response to impacts, forces, accelerations, displacements occurred during the crashes and measuring the human injury possibilities. Transducers, which can be placed on suitable parts of the dummy, give information about physical levels experienced by the dummy. Controlled and repeated crash tests and physical level readings help vehicle designer to improve his design in terms of safety. Similarly to the crash test, in falls it is not possible to use human subjects in falls, given that subjects might get injured and it would be hard to collect consistent data due to varying physiological responses of subjects to the fall. Hence, usage the crash test dummy seems reasonable, given that it increases the safety and allows easy different fall orientation arrangement [10].

The dummy used in our tests is 170 cm tall and 104 kg in weight (Figure 2). The dummy falls on the surface of a force platform, designed in order to have a frequency passband of 40 Hz. In another thesis our colleague focused on the identification of fall data starting from sensors placed on the ground (force and vibration measurements).

The dummy has no ability to stand itself so a lifting construction was created near the platform in order to lift it up and keep it in the standing position. Dummy was hanged to the lifting mechanism by means of a hook placed on the top of the dummy head and a screwdriver as shown in Figure 3. By removing the screwdriver from the hook, friction free falls with very low external influence are obtained.

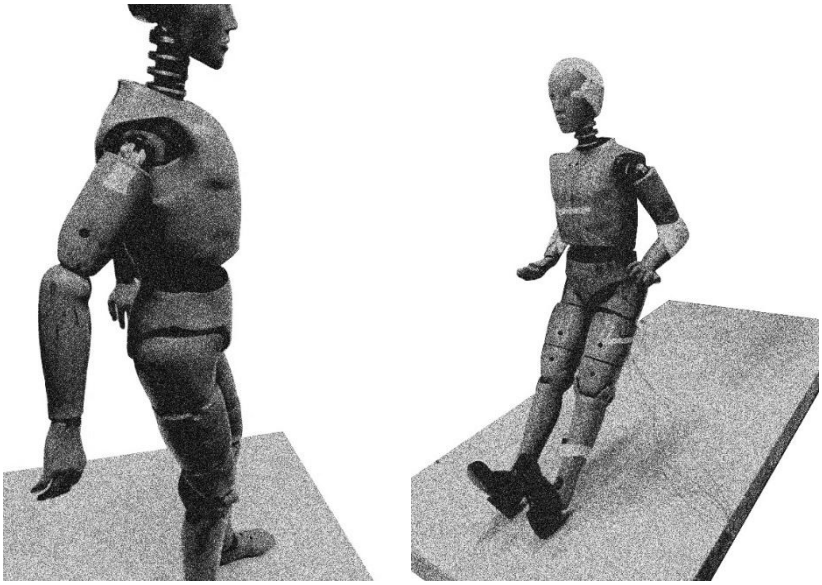

Figure 2 *Dummy used in the tests*

Figure 3 *Quick release mechanism applied*

Three accelerometers were used in our test. One triaxial accelerometer, PCB 356A22, was placed in the head, another triaxial accelerometer, PCB 356A70, was placed on the torso and one mono-axial accelerometer, B&K 4397, placed on the abdomen. The accelerometers location and the measurement axes are shown in Figure 4. The accelerometers are mounted on the metal frame of the dummy by methyle cyanoacrylate, which allows reliable acceleration measurement up to above 1000 Hz, i.e. a value much larger than the interesting frequency range; although there are no standards specifying the bandwidth for this kind of measurements, existing works usually focus on the 0-100 Hz band.

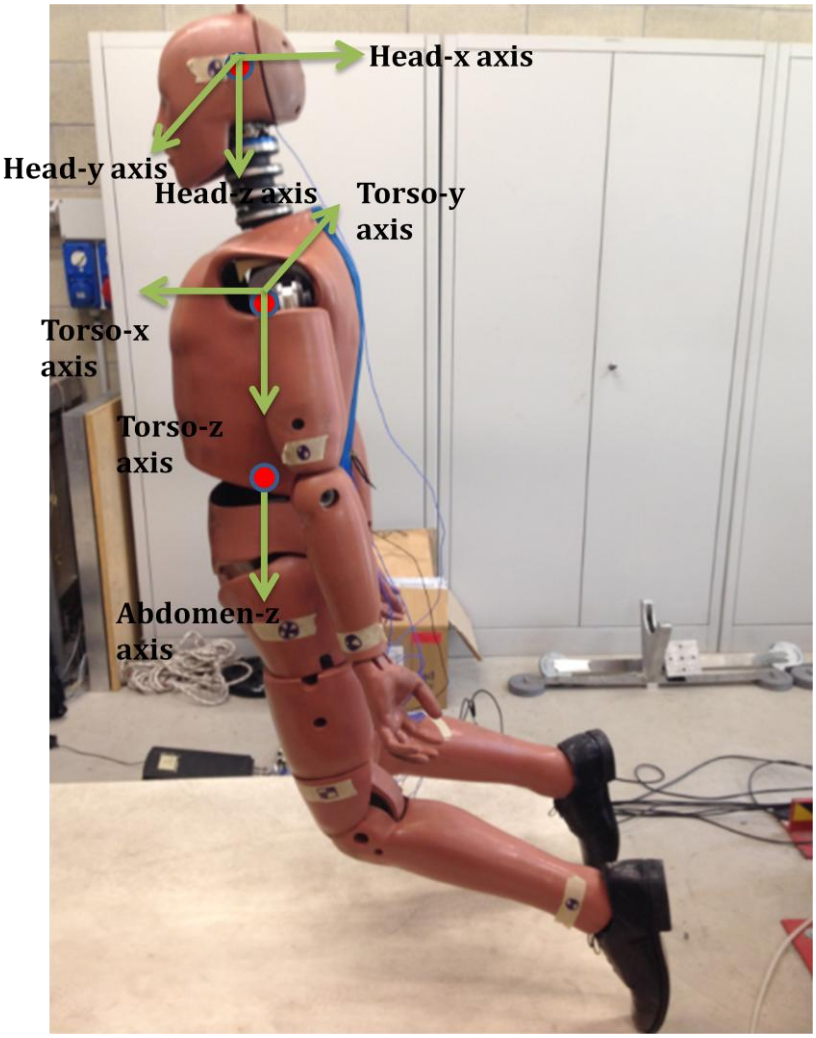

Figure 4 *Placement of accelerometers and their axes*

The accelerometers data were sampled by a National Instrument data acquisition board, ($\pm$10V, 24 bits converter, sampling frequency of 2500 Hz, Antialias filter). The sampled signals were stored on a personal computer and off-line analysed with fit-to-purpose routines implemented in Matlab. The general arrangement can be seen in the Figure 5.

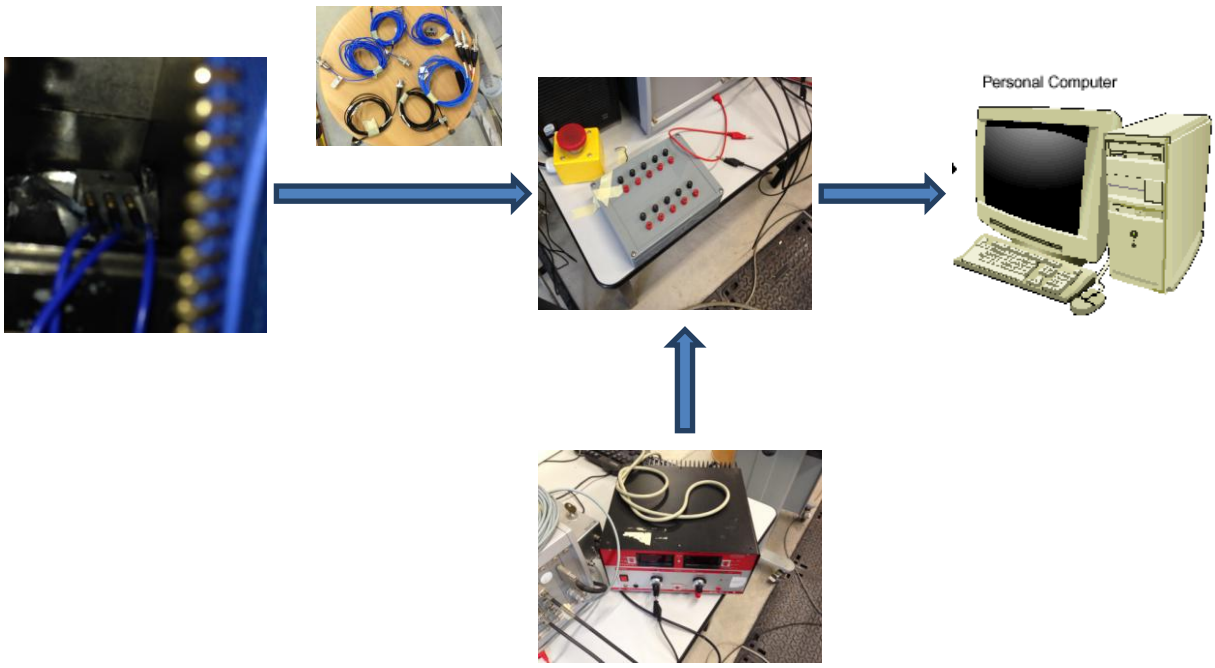

Figure 5 *Connection of the devices for data acquisition*

A video of every test was recorded with a Canon DLSR 550D camera with a 10mm Canon f3.5 wide-angle lens. The camera was located in order to observe the distinctive movement on front-back and up-down direction of the dummy. Exact location of the camera in the test environment is shown in the red circle in Figure 6. The videos were recorded to help understanding the fall kinematic and to allow the computation of the segments trajectories using image processing.

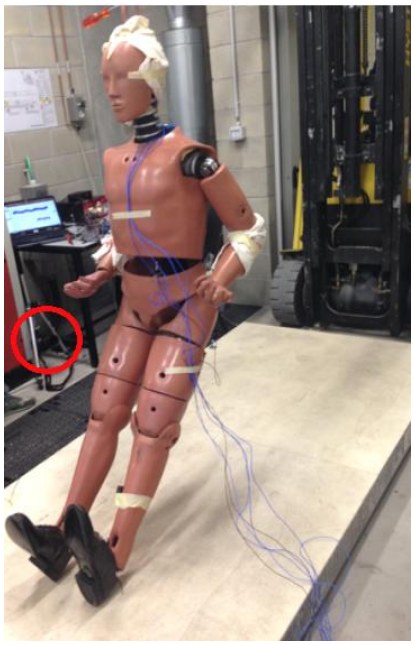

Figure 6 *General test setup and place where the camera is placed*

2.1.2 Experimental Procedure

In order to identify the acceleration of each part during the fall, more than 50 fall tests were performed (forward, backwards and side falls upon varying the influencing factors such as the leg posture or the feet distance). Fall strategies were identified with the help of engineers and doctors of Fondazione Don Gnocchi, which researched for more than ten years acceleration measurements of elders fall. All the falls were recorded by the camera. The junction friction could be set up by tightening the joints of shoulders, elbows, knees and wrists. The test configuration was defined by the following influencing factors:

- Fall direction (forward, backward, side fall)
- Upper limbs posture (one arm arrest, two arms arrest, no arm arrest)
- Fall height: 50 cm, 60 cm, 70 cm, 80 cm (the distance between the ground and dummy buttocks)
- Fall trajectory (free fall or disturbed fall over chair)
- Feet distance: 20 cm, 30 cm (the distance between the middle of heels)
- Pre-fall condition (standing or sitting)

Each fall was repeated two or three times. Falls were named as follows

Type of fall:

- *Rear fall* -R-
- *Front fall* -F-
- *Side fall* -S-

Pre-fall condition:

- *Standing* -1-
- *Sitting* -0-

Height of fall:

- *50cm* -5-
- *60cm* -6-
- *70cm* -7-
- *80cm* -8-

Limbs arrest posture:

- *No arrest* -0A-
- *One arm arrest* -1A-

- *Two arms arrest* -2A-
- *Elbow arrest* -2E-

Legs pre-fall posture described by displacement among the feet:

- *30cm* -3-
- *20cm* -2-

Description of fall trajectory:

- *Free fall (free trajectory)* -F-
- *Fall over the objects (disturbed trajectory)* -D-

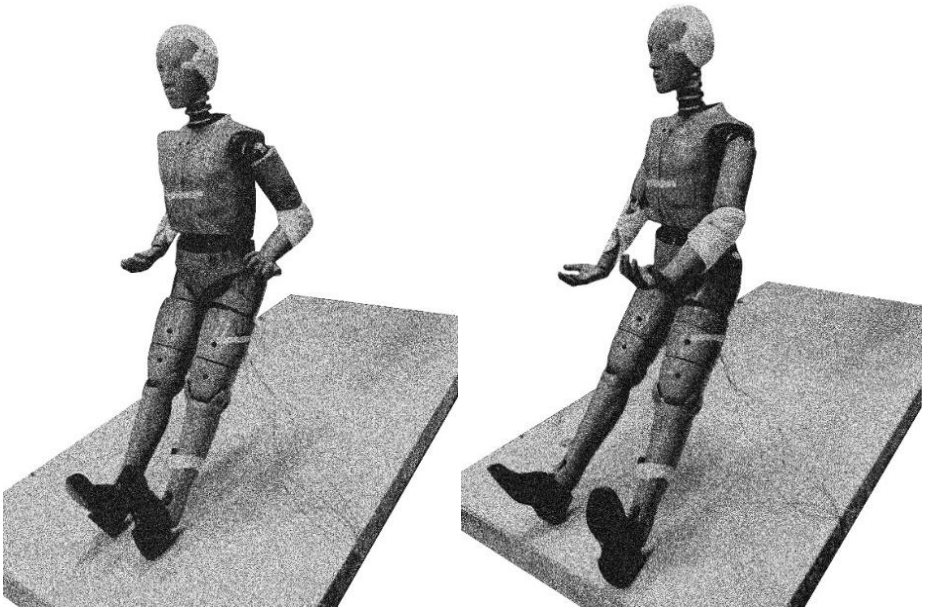

Figure 7 *Positions of the dummy just before quick release for R-1-7-2E-2-F (left figure) R-1-7-0A-3-F (right figure) tests*

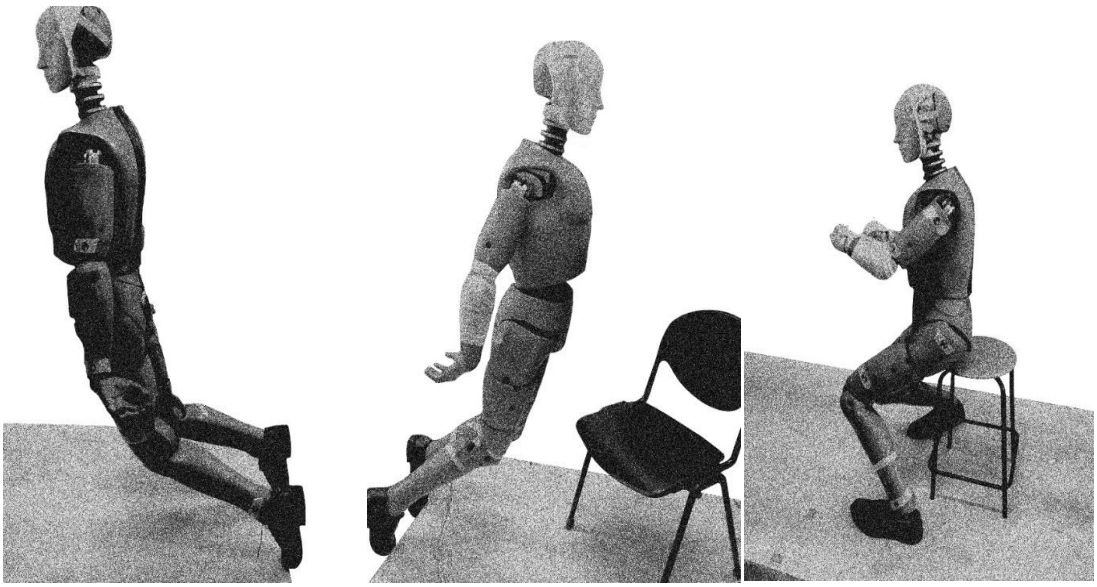

Figure 8 *Positions of the dummy just before quick release for F-1-5-0A-3-F (left figure), F-1-5-0A-3-D (figure in middle), F-0-5-0A-3-F (right figure) tests*

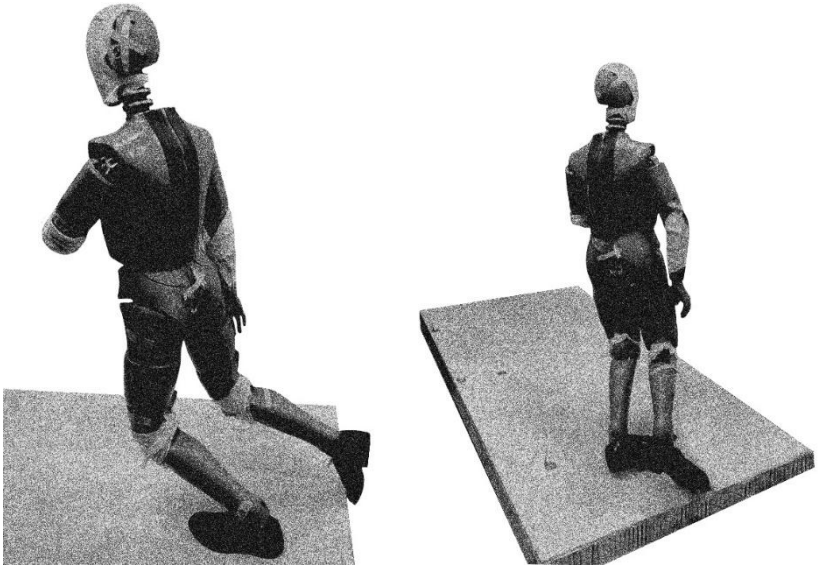

Figure 9 *Positions of the dummy just before quick release for F-1-6-1A-3-F (left figure), S-1-6-1A-2-F (right figure) tests*

2.1.3 Experimental Data Analysis

Acceleration data was offline analysed in order to derive synthetic parameters (indexes) summarizing the entire time history. Time histories were initially triggered in order to extract only the significant part of the signals. All the acceleration time histories were triggered with 7000 samples and a pretrigger of 2000 samples. In this way, the time length of the signal was large enough to include all the tests. With the adopted

procedure, said x(t) the acceleration, the trigger time history is obtained by taking 2000 samples before the trigger level TL. The trigger time is the time t* for which:

$$x(t^*)=TL$$

Data (originally sampled in a binary format) were exported in .mat file by a fit-to-purpose MATLAB script. A logic using three-dimensional matrices was created on MATLAB. This allows us to categorize and manipulate the data for each test and each time history. In our 3D matrices, we have a row indicating the number of the test, the column indicating the acceleration values versus time and the page indicates the accelerometer and the axis that we are interested in. As an example:

$$A(30,:,3)$$

has the 7000 elements pointing the acceleration values of each sample (at each time step) of triggered data for the z axis of the head at the 30th test. Last number in the designation, in this example it is 3, indicates interested accelerometer and the axis of it. By changing the column in the middle, we can also find exact acceleration value for the number of sample that we want.

After the creation of 3D matrices, data was filtered by Butterworth low-pass filter of 4th order at 300Hz. The cut-off frequency was dictated from the necessity of including high frequency components in the study of the dynamics of the floor (included in another thesis on the same topic). The filtered time histories were used to derive the peak accelerations in x-y-z directions of the head, x-y-z directions of the torso, and z direction of the abdomen are found for each test. Additionally, the resultant acceleration of the head was also calculated.

$$a_R = \sqrt{a_x^2 + a_y^2 + a_z^2}$$

Peak accelerations were analysed with Excel and Minitab. Each of the videos taken during the falls was cut according to the start/end time of related fall. In this way, we could have just falling parts on the videos to operate them on MATLAB for video processing and fall time analysis.

2.2 Peak Acceleration Analysis

The main purpose was to make inferences about the effects of the influencing factors on the peak accelerations. So considering 3 main groups of the fall type (forward, backward, side), the boxplots of peak accelerations for x-y-z directions and resultant of

the head and x-y-z directions of the torso were plotted with respect to variation of each factor. The boxplots provide us information about the range of the peak accelerations and its median corresponding to the specific groups of a pre-determined factor. The signals obtained from accelerometer placed on the abdomen were indicating non-realistic acceleration due to a possible damage of the cable and data was not analysed.

2.3 Falling Duration Analysis

Falling time duration can be defined as the time interval between start and end of a fall. It might depend on many factors describing the dummy's initial posture and the environment where falls happen. In our study, the falling durations of all tests were estimated by three different approaches. The reliability of the three approaches was compared and the best one was chosen in order to carry out further analysis.

The first approach for determination of the falling time was based on a subjective evaluation of the event length; for each fall, we observed the triggered acceleration time histories as in Figure 10 and Figure 11, and fall duration was estimated by subtracting the end time from the start time. This procedure is applied for all tests.

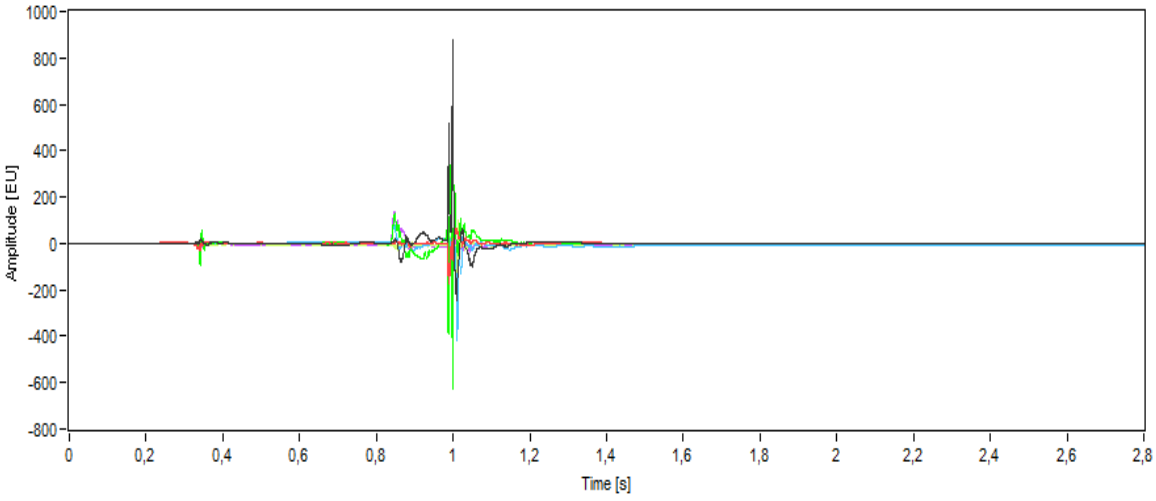

Figure 10 *Triggered acceleration-time histories of the head (x-y-z direction) and the torso(x-y-z direction) on one plot for R-1-8-0A-2-F test*

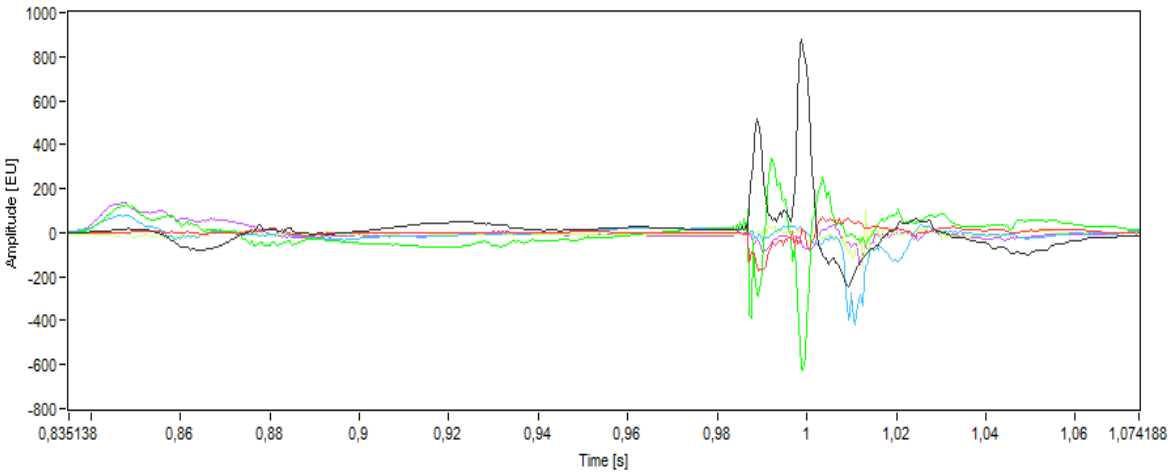

Figure 11 *Zoomed acceleration-time histories of head (x-y-z) and torso(x-y-z) on one plot for R-1-8-0A-2-F test, start and end times of the fall*

The second approach also uses the acceleration-time histories to find falling duration. For this case, time histories were analysed with MATLAB. After maximum peak value was found on each accelerometer axis, we stored the first and last time in which the signal was above 10% of maximum value. Falling durations per axis of each accelerometer were averaged to obtain unique falling duration for each fall. In general, differences between the durations of each axis were limited. A unique threshold was used in all the tests, in order to reproduce what actually happens in the fall detection, where a unique trigger level is used for all the events. The trigger level was set to 15 m/s^2. This value allowed discarding from the duration the vibration of the dummy generated by the manual quick release mechanism. The adoption of lower trigger levels lead to errors in the estimation of the time length because of the inclusion of this spurious event at the beginning of the time history.

The last approach exploits the videos that are taken for each fall. On MATLAB, it is possible to convert the video files (in our case *.wmw files) into the sequence of frames. Some of the frame images for a free backward fall can be seen in the Figure 12.

The frame rate of the video files was known from the specifications of the video. All videos have a frame rate of 30 frames/s. The falling duration can be determined by multiplying the constant time difference between consequent frames (1/30 [s/frame]) with the number of frames between the frame that first movement of the body due to fall is seen and the first frame which the movement of the body stops totally.

Figure 12 *Frames showing postures of the dummy during a free backward fall*

The last approach considers the fall from the very beginning (instant when the subject starts moving from upright position) to the very end (instant when the subject rests on the ground) and therefore is usually larger than the others. Since in the video processing there is no ambiguity related to the presence of minor events it was chosen to analyse data computed with this method.

2.4 Video Processing

The first objective of video processing is to obtain the trajectory of the body parts. Knowing trajectory of different parts might be beneficial for the understanding how different parts of the body are physically affected during the fall. The other objective is to obtain velocity values by video processing in order to investigate the correlation between the data obtained from video and from accelerometers. In this way, an estimation about velocity and acceleration of the body parts could be done by analysing just the videos.

At first, we tried to obtain the data by use of pattern recognition for the head. However, some problems were encountered. When the frames of the videos observed one by one,

it was seen that there are many blurry images of the head and other body parts on some frames, since its high velocity during the fall and the insufficient lightening of the test environment. Blur generally occurs when camera has not short exposure time and it causes complication for automatic detection [11]. Therefore, the strategy was shifted from automatic processing to manual processing. Instead of pattern recognition for traction, we have worked frame by frame to mark a small certain area of regarding part to obtain the trajectory of that part. Manual processing gave the advantage that the tracked spot can be guessed and marked even in case of blur presence in some frames.

Using frame-by-frame marking of tracked point on the dummy, we could obtain the coordinates of the signed point in pixel. Frame-by-frame tracked points on the dummy for a forward fall from the sitting position can be seen in the Figure 13.

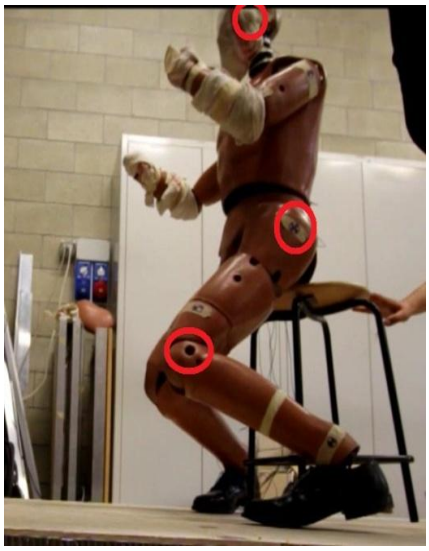

Figure 13 *Tracked spots on the dummy*

The real displacement values between signed points were found by using a factor to pass from pixel to m. Using the real heights of the objects on the video plane, the image sensitivity was measured. In our case, the sensitivity was determined from the chair height, (0,60 equivalent to 266 pixel).Although more complex algorithms are available, the adopted method was found to be robust. The real-world trajectory of the body segments was obtained; samples of trajectories are shown in the Results section.

Knowing the frame rate of the videos, the velocity-time characteristic of the tracked part on the x and z directions of the videos plane was calculated by dividing the distance on x and z directions between two consequently marked points by time between two frames, which is 1/Frame rate.

Since accelerometers' axes are rotating with respect to the videos axes, the comparison between the velocities obtained from video processing with those obtained by

integration of acceleration-time history had to include the rotation. The latter was derived from the video processing. The head tilt was measured from an angle defined by two fixed points as in Figure 14. Velocities on the video plane were converted to velocities on accelerometers plane by using this angle for each frame.

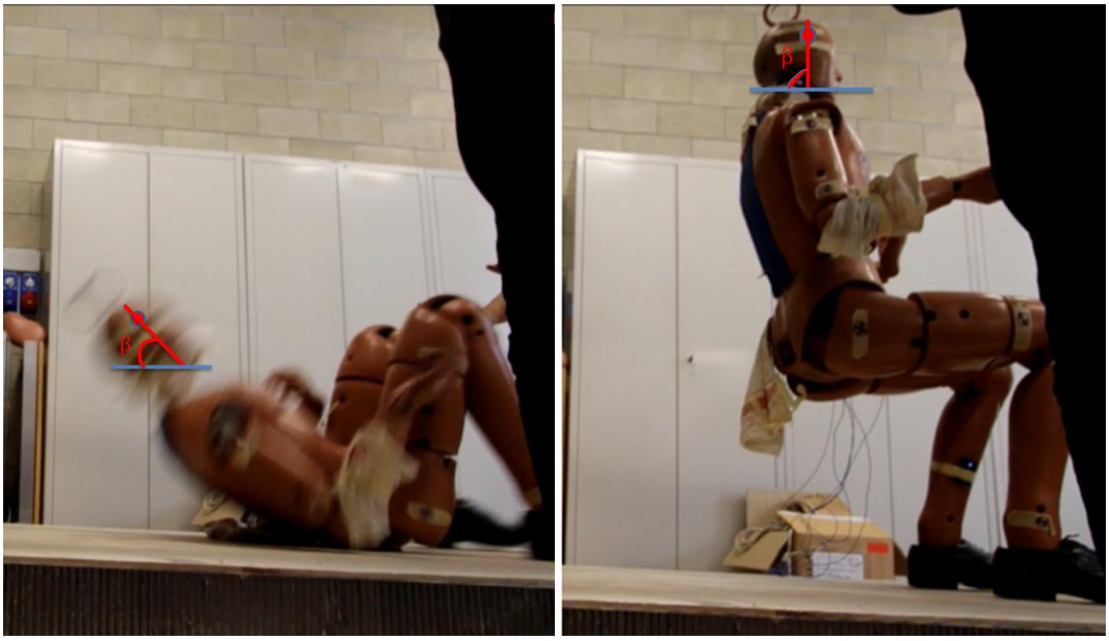

Figure 14 *Angle between vertically defined line on the head with respect to stable x axis of the video plane*

Considering that $V_{x\_head}(i)$ and $V_{z\_head}(i)$ are the velocity of the head on the video's stable x and z axes and $V_{x\_head}*(i)$ is the velocity of the head on the accelerometers rotating x axis:

$$V_{xhead}*(i) = \sin(\beta) * Vx\_head(i) + \cos(\beta) * Vz\_head(i) \quad \text{for the backward falls}$$

$$V_{xhead}*(i) = -\sin(\beta) * Vx\_head(i) - \cos(\beta) * Vz\_head(i) \quad \text{for the forward falls}$$

"i" is the frame number. The velocity curves were de-noised using the CSAPS function in MATLAB starting from the discrete velocity values [12]. The smoothing parameter "p" can have values between zero and one, and it determines the relative weight we would like to place on the contradictory demands of having a function be smooth versus having a function be close to the data. If p=1, obtained curve is perfectly close to the data but it is not smooth. If p=0, the curve is smooth but so far from the discrete data. P was set to 0.3, a value granting a good compromise between the smoothness and the correspondence with the physical phenomena; we must account that the noise is mainly due to the difficulty of choosing the same point in consecutive frames in blurry images, so the filtering procedure is always necessary.

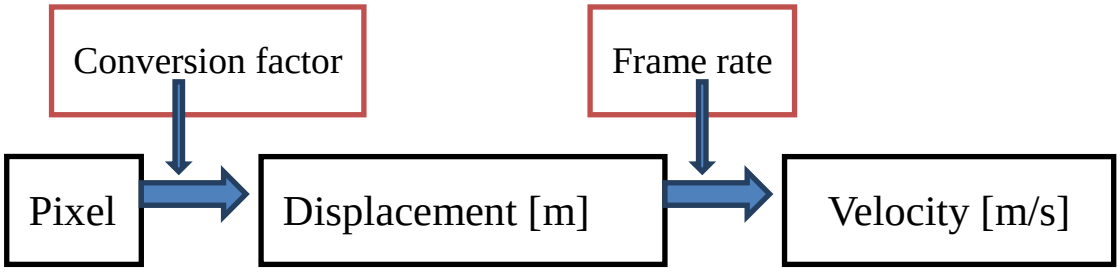

Figure 15 *Scheme of the logic used to obtain velocity on the rotating x axis of the head by video processing for comparison with the velocity obtained from the accelerometer*

Trajectories and velocities on the rotating x axis of the head are obtained by the method described above. Twenty-one videos (tests) were processed. Moreover, the velocity graphs of the head on rotating x axis were found by integration of the acceleration-time histories on the x axis of the accelerometer placed on the head. For each test, the peak value of the velocity obtained from video processing and the velocity obtained from integration of acceleration data is compared. Error and root-mean-square error were computed and used as figure of merit for the video trajectory.

Lastly, two random falling videos found on the internet were processed in order to show that the approach could be also beneficial to have information about physical quantities and their changes in the real conditions without usage of accelerometers. The problems affecting reliability of the results are afterwards discussed.

3 Results

3.1 Peak Acceleration Analysis

Acceleration-time histories of the head and torso on x-y-z directions for a test (R-1-8-0A-2-F) are shown as an example in Figures 16 to 21.

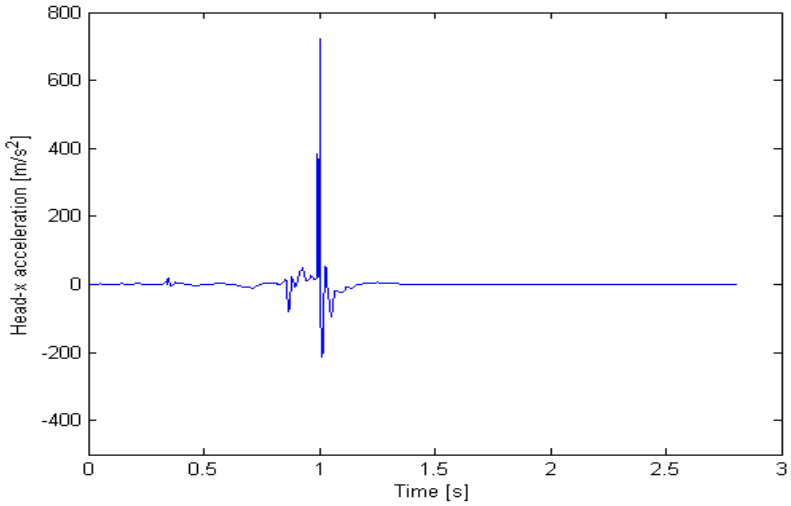

Figure 16 *Acceleration-time history of the head on x axis of the accelerometer for R-1-8-0A-2-F test*

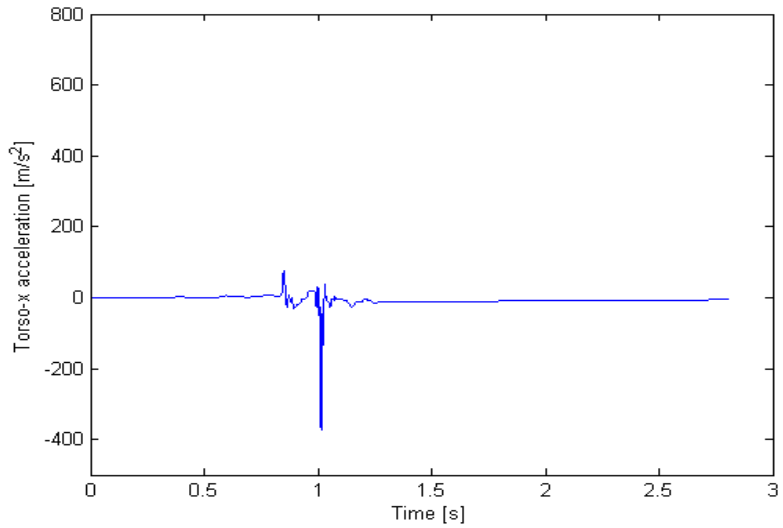

Figure 17 *Acceleration-time history of the torso on x axis of the accelerometer for R-1-8-0A-2-F test*

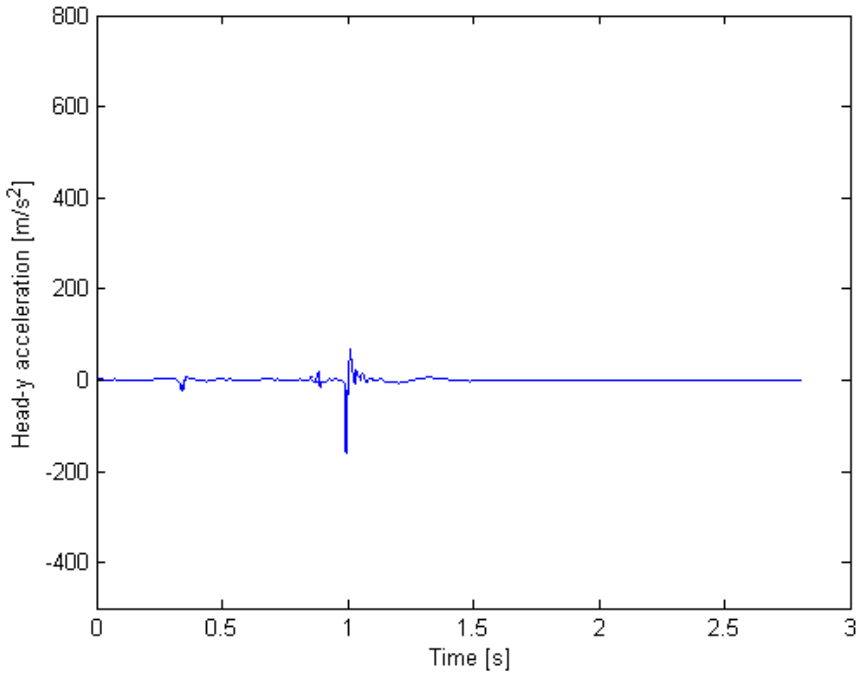

Figure 18 *Acceleration-time history of the head on y axis of the accelerometer for R-1-8-0A-2-F test*

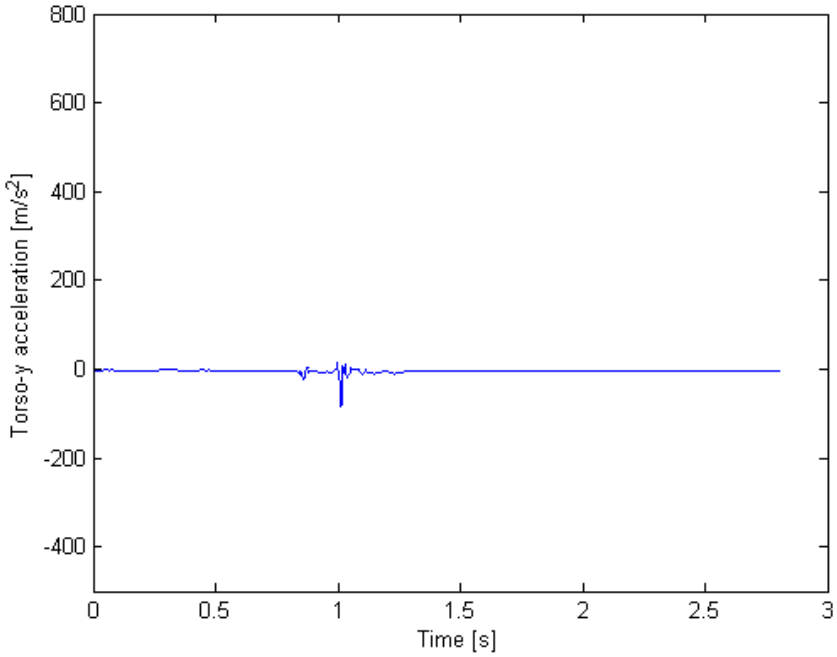

Figure 19 *Acceleration-time history of the torso on y axis of the accelerometer for R-1-8-0A-2-F test*

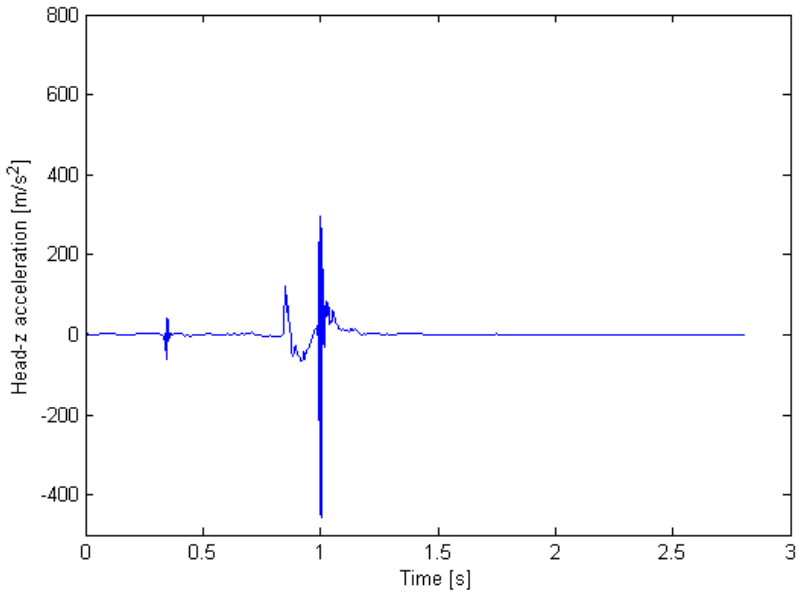

Figure 20 *Acceleration-time history of the head on z axis of the accelerometer for R-1-8-0A-2-F test*

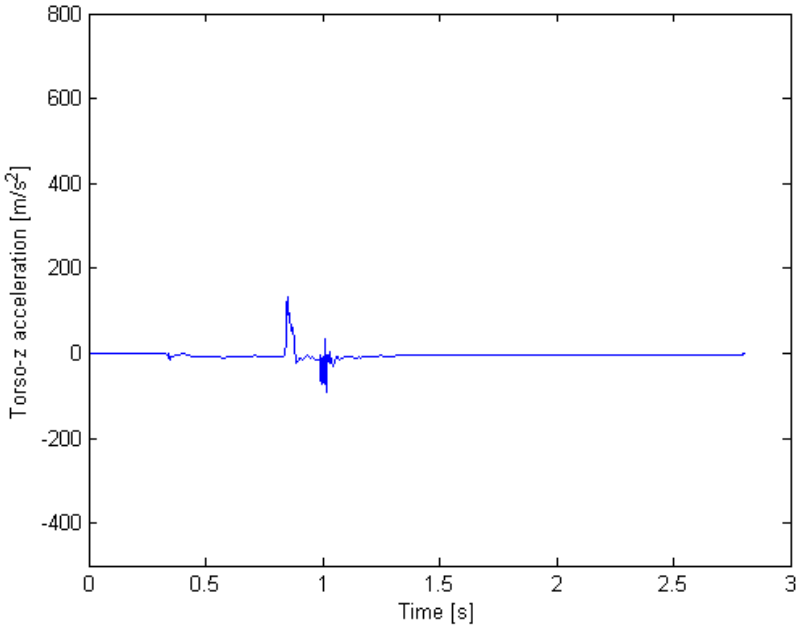

Figure 21 *Acceleration-time history of the torso on z axis of the accelerometer for R-1-8-0A-2-F test*

It can be observed that, in this particular case, the head has experiences higher accelerations compared to the torso, but data are difficult to interpret. Results were therefore summarized by boxplots by grouping the influencing factors.

3.1.1 Arm Arrest Effect

The effect of arm arrest on the head acceleration in backward falls is shown in Figures 22 to 24. It can be stated that absence of arm arrest during the fall causes higher peak acceleration on each axis of the head and naturally on the resultant acceleration. Highest peak values with loose arms were reached on x axis of head. Data clearly show that falls without arm arrests are more dangerous for the head with respect to arm arrested ones. Acceleration values of the torso were affected by saturation and therefore not analysed.

For the forward fall group, two-arm arrested falls were done by closing the arms on the chest. In this case, a large data variability occurs without arm arrest, although the average values are similar. Boxplots of the head accelerations are shown in the next page.

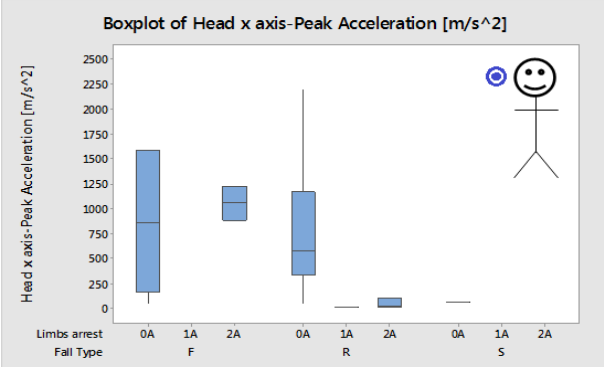

Figure 22 *Peak acceleration boxplot of the head on x axis for varying arm arrest condition per type of fall*

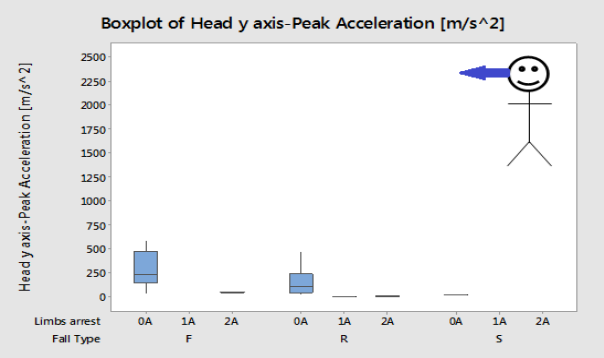

Figure 23 *Peak acceleration boxplot of the head on y axis for varying arm arrest condition per type of fall*

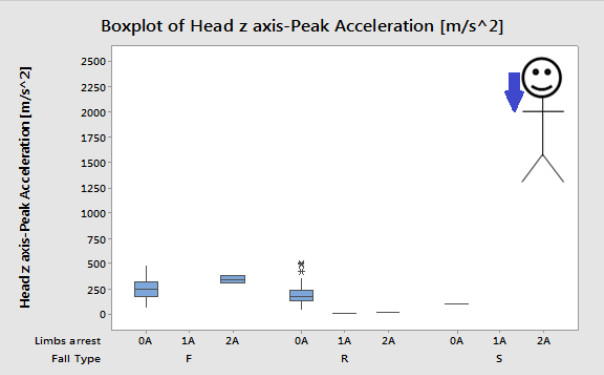

Figure 24 *Peak acceleration boxplot of the head on z axis for varying arm arrest condition per type of fall*

The accelerations along the x axes are always larger than those measured along the y and z axes. The variability was generally low, except with the “no arrest” in front and backward falls. The comparison between two-arm arrested front falls with the one in which there is no arm protection is shown in Table 1.

Nomenclature						Head-x axis	Head-y axis	Head-z axis	Head-Resultant	Torso-x axis	Torso-y axis	Torso-z axis
F	1	8	0A	3	F	1595	587	180	1705	177	58	130
F	1	8	0A	3	F	1597	383	302	1667	170	43	115
F	1	8	2A	3	F	1235	56	387	1281	143	26	159
F	1	8	2A	3	F	883	43	312	930	110	53	111

Table 1 *Comparison of 2A forward falls' maximum accelerations [m/s^2] with the falls having same pre-fall conditions except their arm arrest condition that is 0A.*

The two arm arrested falls have lower resultant head acceleration with respect to no arm arrested falls and it means that arm arrest prevent head from reaching higher acceleration values. Furthermore, x axis of the torso is more severe than y and z axis in terms of acceleration, also has lower maximum acceleration values in case of two arm arrested front falls. In some "two arm arrested" falls the acceleration on the three axes are comparable; since arm arrest is obtained by closing the arms on the chest, it's more effective on x direction of the head but this may induce higher accelerations on z direction. For the backward falls, arm arrests are applied by completely opening the arms and tightening the screws at the elbow, so hands are touching the ground first and starts to damp the fall earlier. This might be the reason that we have lower maximum acceleration values on the z axis of the head in case of arm arrested backward falls.

General inference about the head can be made by considering distribution of maximum head resultant acceleration in the Figure 25. Since one axis is dominant with respect to the others, the information about the resultant acceleration is very similar to that of the x axis.

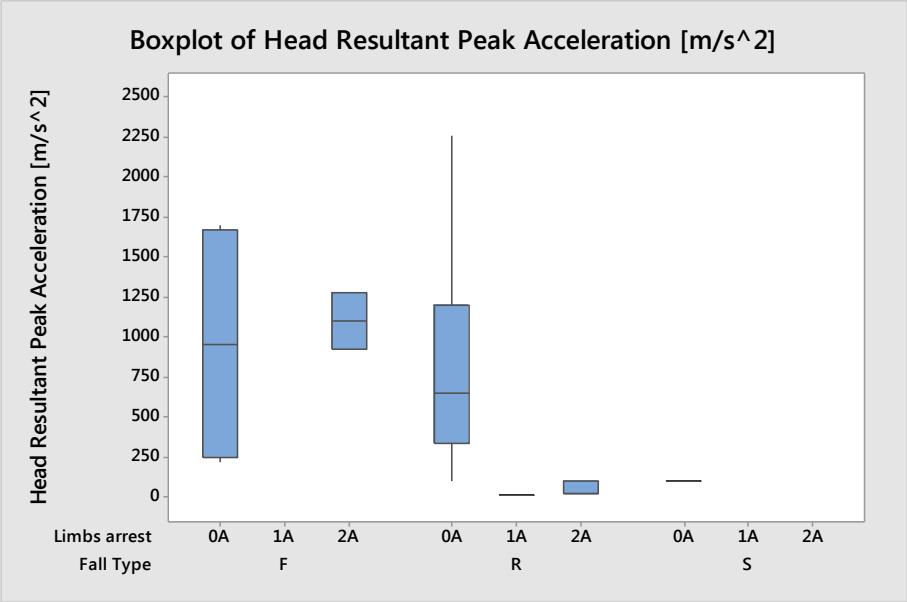

Figure 25 *Peak acceleration boxplot of the head resultant for varying arm arrest condition per type of fall*

The acceleration on the torso was measured only in a limited set of configuration, owing to measurement artefacts detected in the signal; only forward falls will be discussed.

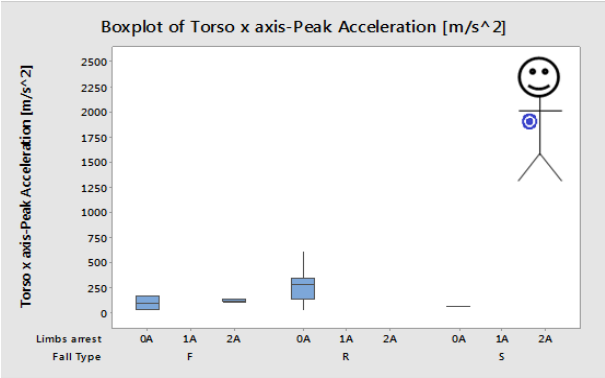

Figure 26 *Peak acceleration boxplot of the torso on x axis for varying arm arrest condition per type of fall*

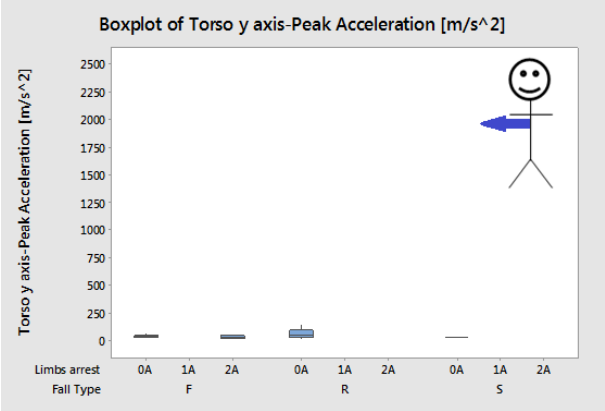

Figure 27 *Peak acceleration boxplot of the torso on y axis for varying arm arrest condition per type of fall*

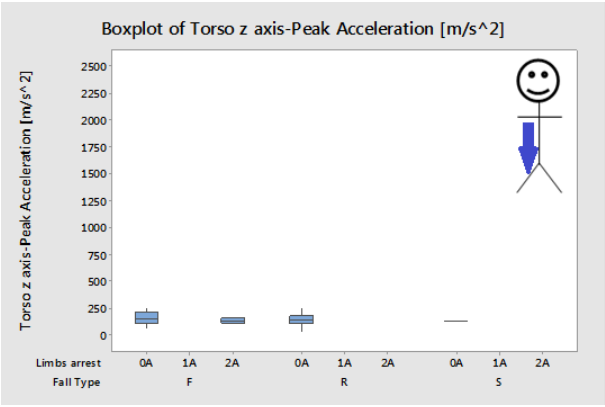

Figure 28 *Peak acceleration boxplot of the torso on z axis for varying arm arrest condition per type of fall*

Boxplots show that accelerations are generally comparable, although the x acceleration is larger than the others as in the majority of the situations presented in this thesis.

3.1.2 Falling Height Effect

The fall height is summarized in figures from 30 to 36; the effect of the height has on the peak acceleration is relevant, especially on the x axis of the head.

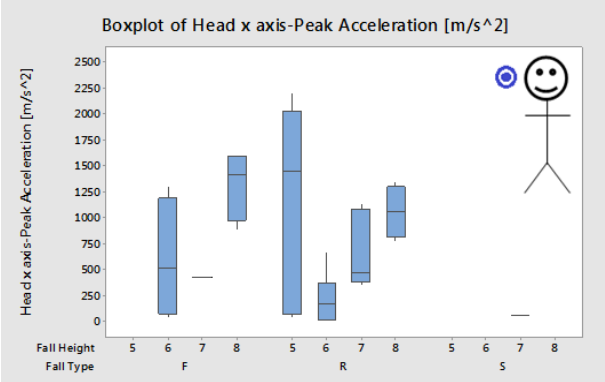

Figure 29 *Peak acceleration boxplot of the head on x axis for varying falling height condition per type of fall*

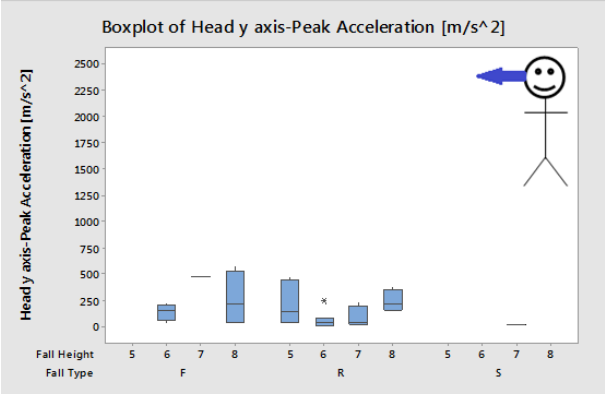

Figure 30 *Peak acceleration boxplot of the head on y axis for varying falling height condition per type of fall*

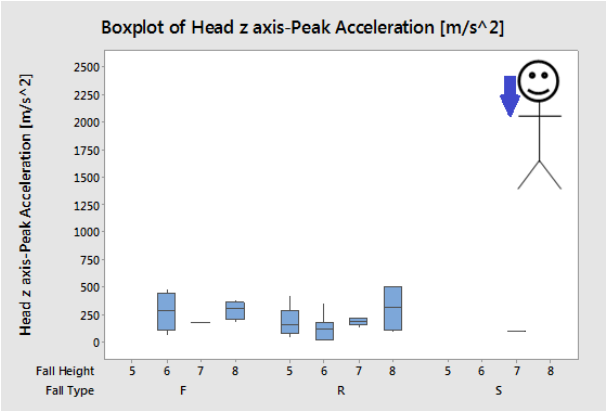

Figure 31 *Peak acceleration boxplot of the head on z axis for varying falling height condition per type of fall*

The rear falls with 50 cm distance between hips and the platform lead to larger head-x and head resultant peak acceleration values. The reason of this behaviour was found observing the videos: given that the distance between the ground and the hips is very low, hips do not touch the ground entirely, and consequently movement of the head is not interrupted until the fall ends. When the height increases, hips are clearly hitting on the ground during the fall and the deriving acceleration increases as expected; this can be explained observing the kinematics of the fall indicated in Figure 29. The contact between calf and thigh produces damping to prevent crushing of hips to the ground. By the heights of 60 cm and higher, calf is tilted. Thus, the angle between calf and thigh is becoming higher and it causes less damping. Also with increase in height, the damping due to contact of dummy parts starts relatively later and the absorbed energy decreases. With the heights of 50 cm and lower, angle between calf and ground becomes reverse; therefore, thigh and hips muscles (friction between the joints in our case) can be large enough to prevent crushing of hips to the ground.

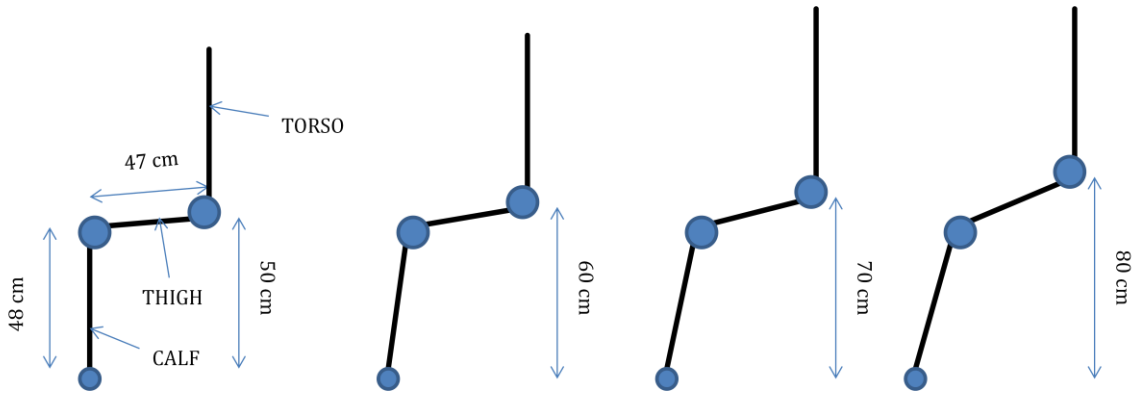

Figure 32 Positions of the calf, thigh and torso for each fall height

The resultant acceleration is shown in Figure 30.

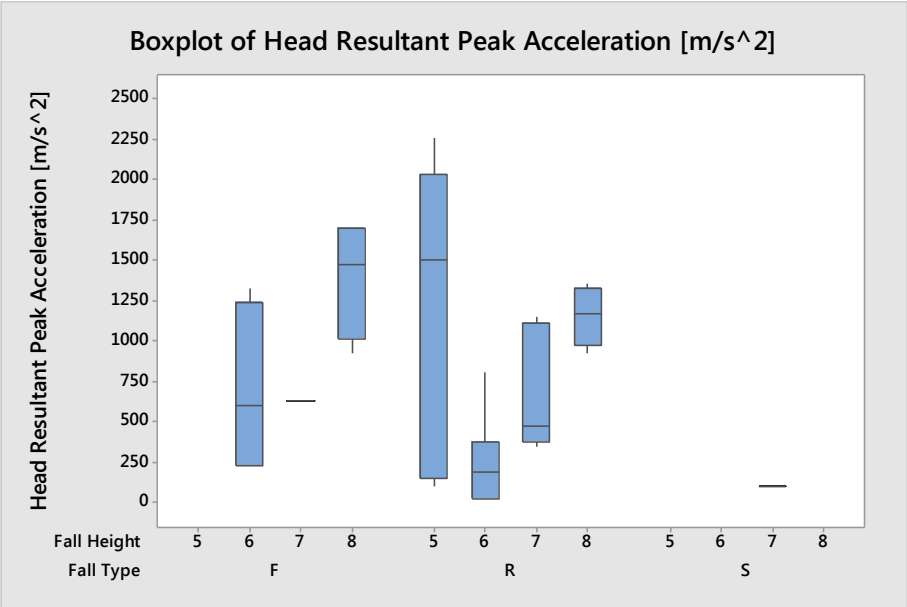

Figure 33 *Peak acceleration boxplot of the head resultant for varying falling height condition per type of fall*

The effect of the fall height on the acceleration at the torso are shown in the next figures

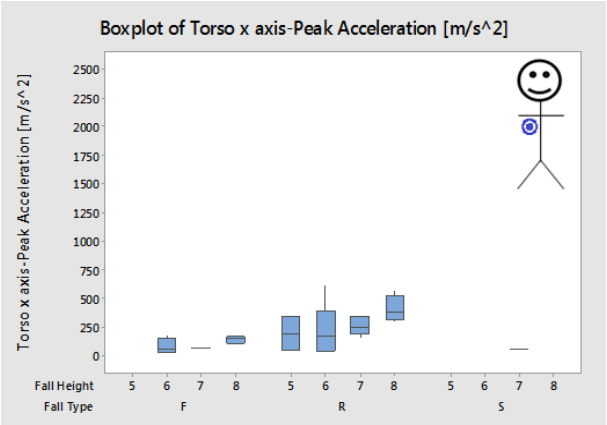

Figure 34 *Peak acceleration boxplot of the torso on x axis for varying falling height condition per type of fall*

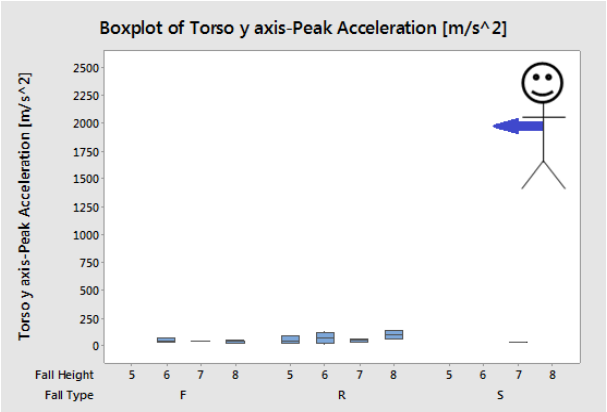

Figure 35 *Peak acceleration boxplot of the torso on y axis for varying falling height condition per type of fall*

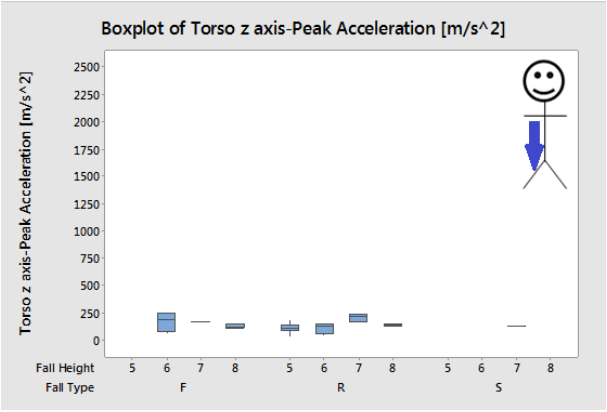

Figure 36 *Peak acceleration boxplot of the torso on z axis for varying falling height condition per type of fall*

In this case, the acceleration are generally low and will not be discussed here.

3.1.3 Falling from sitting or standing posture

Peak acceleration boxplots that are plotted for sitting and standing pre-fall conditions (sitting or standing posture, 0 and 1 respectively) are shown in Figures from 37 to 43. Accelerations at the head are hereafter presented.

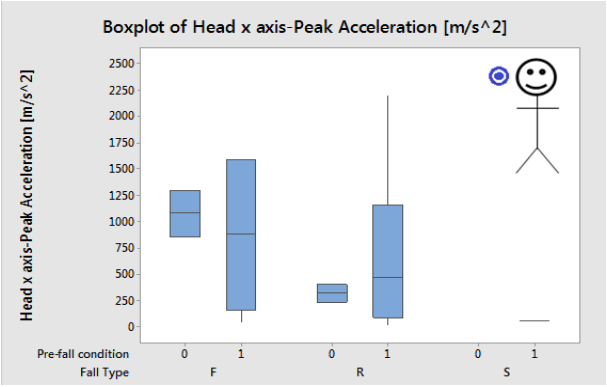

Figure 37 *Peak acceleration boxplot of the head on x axis for varying pre-fall condition per type of fall*

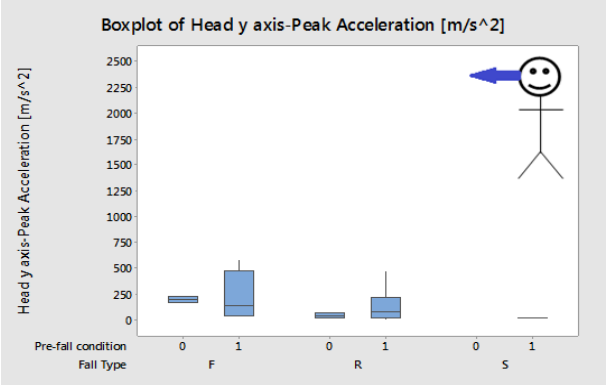

Figure 38 *Peak acceleration boxplot of the head on y axis for varying pre-fall condition per type of fall*

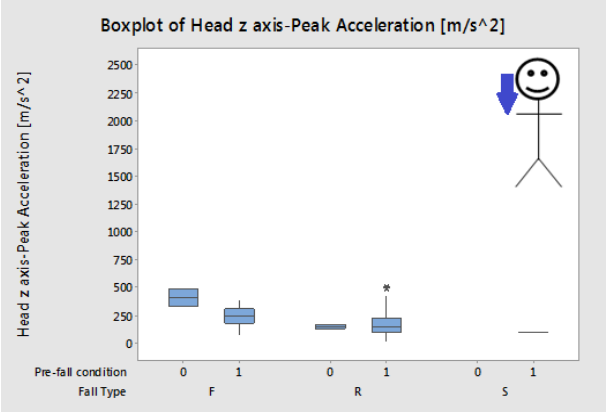

Figure 39 *Peak acceleration boxplot of the head on z axis for varying pre-fall condition*

per type of fall

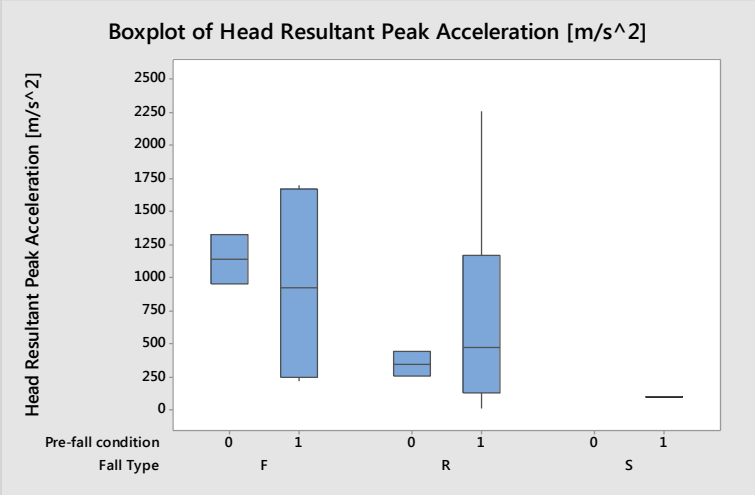

Figure 40 *Peak acceleration boxplot of the head resultant for varying pre-fall condition per type of fall*

The acceleration along the x axis is generally larger than the others and therefore is dominant on the behaviour of the resultant acceleration. The median of the accelerations are generally comparable, but we can identify some regularities in the peak accelerations:

- If the subject is sitting (condition 0) the forward fall leads to a larger acceleration with respect of the backward fall
- If the subject is standing (condition 1) the peak acceleration is averagely larger in forward fall, but the data variability is important.

In this case, the legs play a very important role in the dynamics of the fall, given that in rear falls they are lifted, thus increasing the inertia versus rotation and decreasing the acceleration value. This aspect is clarified in the next figures.

Figure 41 Position of the body parts for the backward falls from sitting position (left figure), Position of the body parts for the backward falls from standing position(right figure)

Figure 42 Forward fall from sitting position

The accelerations at the torso are shown in the next figures.

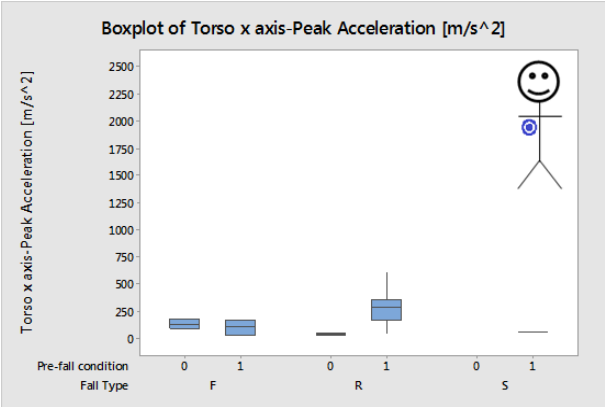

Figure 43 *Peak acceleration boxplot of the torso on x axis for varying pre-fall condition per type of fall*

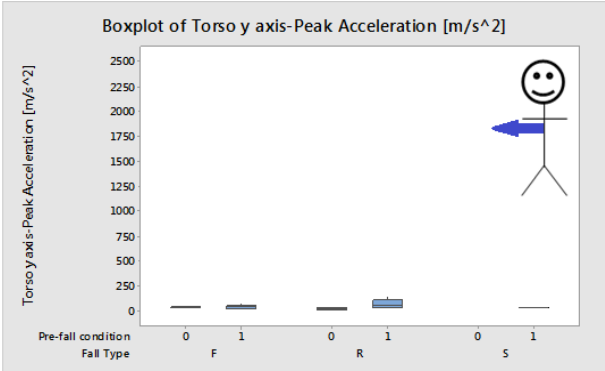

Figure 44 *Peak acceleration boxplot of the torso on y axis for varying pre-fall condition per type of fall*

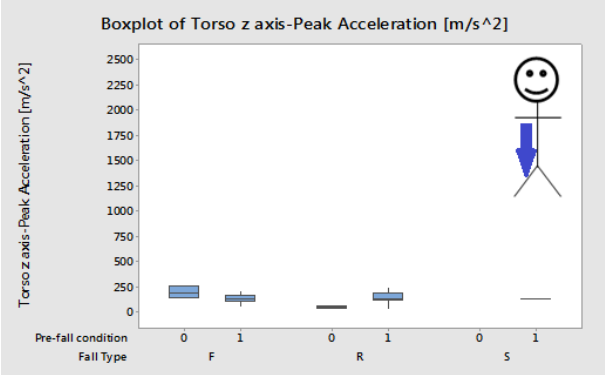

Figure 45 *Peak acceleration boxplot of the torso on z axis for varying pre-fall condition per type of fall*

Accelerations on the three axes are generally comparable and do not depend on the sitting/standing posture. The only noticeable differences occur in rear fall on the x axis, where the acceleration from standing posture is systematically larger than the

acceleration experienced when falling from sitting posture.

3.1.4 Presence of obstacles on the trajectory

The effect of obstacles was investigated by comparing the acceleration of a free fall (F) with those of a disturbed fall (D), where the subject was falling against a chair. Results are summarized in the next plots.

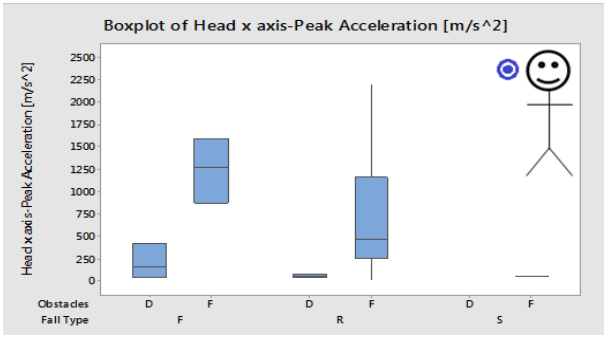

Figure 46 *Peak acceleration boxplot of the head on x axis for varying fall trajectory condition per type of fall*

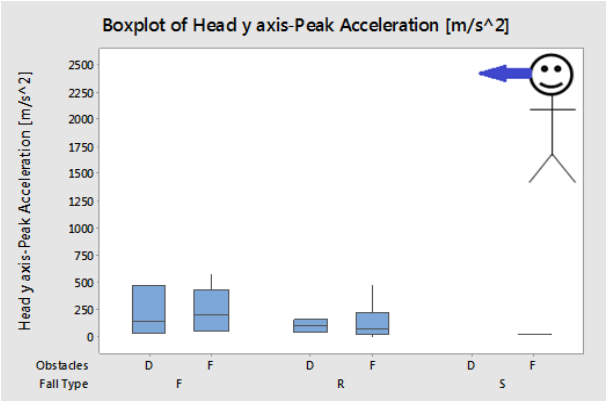

Figure 47 *Peak acceleration boxplot of the head on y axis for varying fall trajectory condition per type of fall*

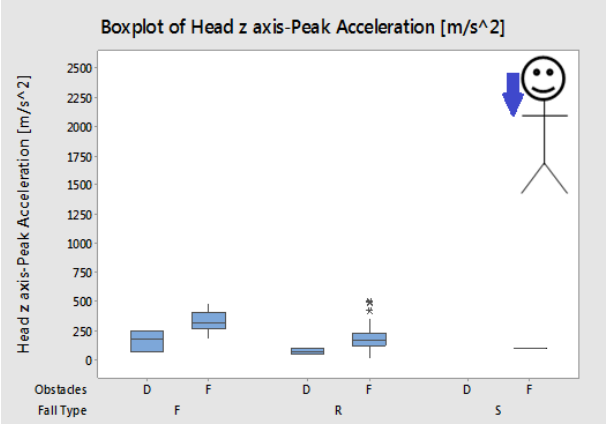

Figure 48 *Peak acceleration boxplot of the head on z axis for varying fall trajectory*

condition per type of fall

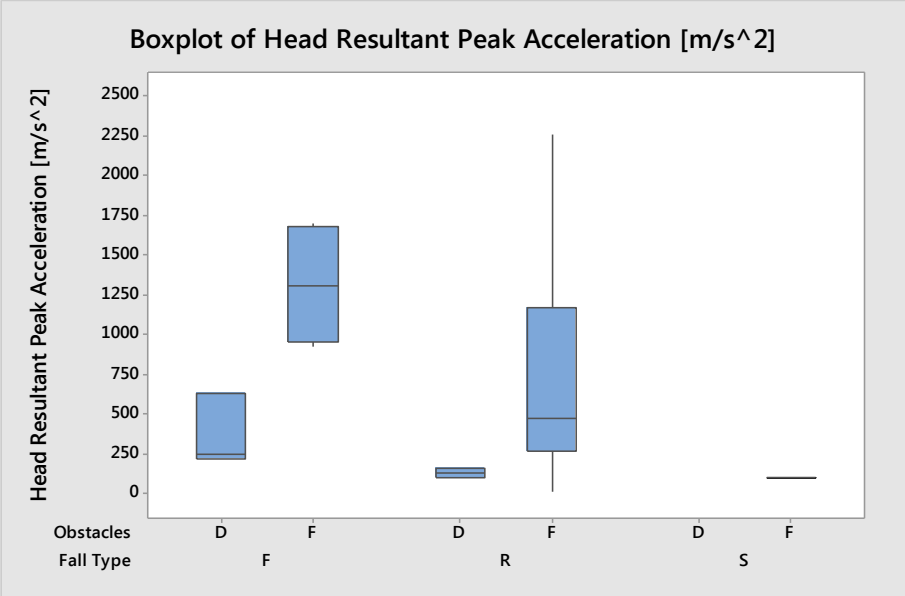

Figure 49 *Peak acceleration boxplot of the head resultant for varying fall trajectory condition per type of fall*

Figure 46 shows that the disturbing effect of the chair largely reduced the head x acceleration for both forward and backward fall types. Figure 47 shows that the maximum acceleration values on y axis of the head are distributed approximately from 50 m/s^2 to 470 m/s^2 for forward disturbed falls and from 50 m/s^2 to 150 m/s^2 for the backward disturbed falls. Besides, lateral accelerations of disturbed and free falls are comparable. Figure 48 shows the z accelerations, which are 75-250 m/s^2 for backward falls and 50-100 m/s^2 for the forward falls

Accelerations at the torso are shown in figures from 50 to 54. Disturbed falls maximum accelerations are generally lower than the free ones.

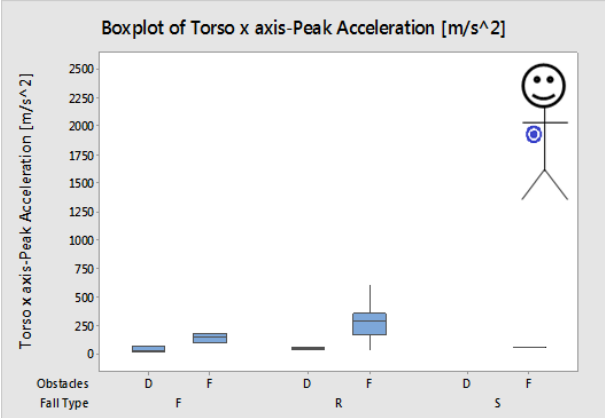

Figure 50 *Peak acceleration boxplot of the torso on x-axis for varying fall trajectory condition per type of fall*

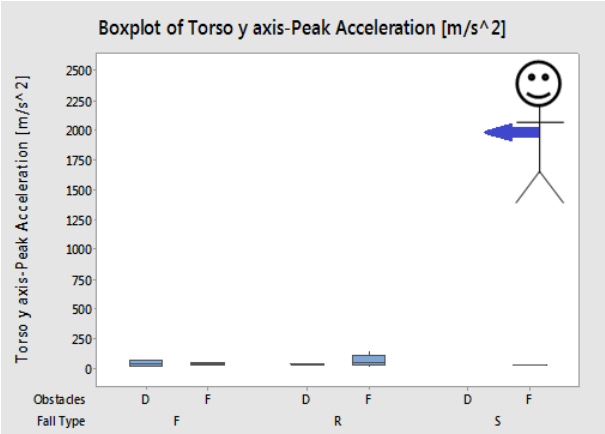

Figure 51 *Peak acceleration boxplot of the torso on y axis for varying fall trajectory condition per type of fall*

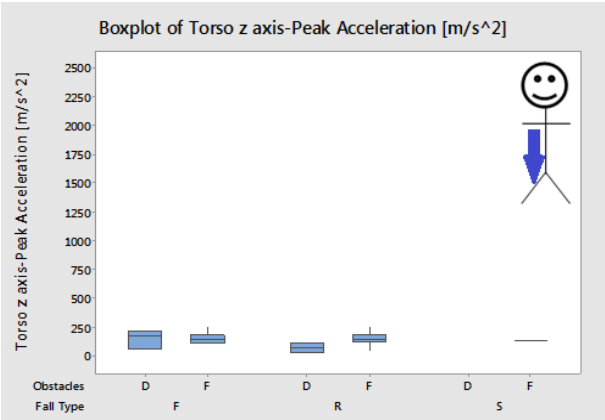

Figure 52 *Peak acceleration boxplot of the torso on z axis for varying fall trajectory*

condition per type of fall

The differences between the front and the backward falls are generally limited, and as in the other cases, the torso values are much larger than the head ones. The contact of the hips with the chair prevents reaching higher maximum acceleration for the backward disturbed falls. For the forward fall, disturbed falls has not clearly lower maximum accelerations compared to forward fall. The probable reason is that the disturbance of the fall may happen after the knees hits the ground, so the disturbance is more effective on the z direction with respect to the x one.

In general, we can state that free falls are more dangerous than disturbed falls, since the peak accelerations are generally larger. In disturbed falls, the velocity of the first impact is generally lower with respect of the free fall causing lower peak acceleration values on head-x and torso-x axes. However, the consideration just takes into account the maximum acceleration value and do not include, for instance, the risk of hitting sharp surfaces or corners. Accelerations on the y and z axes are generally comparable.

3.1.5 Feet Distance Effect

The effect of the feet distance is summarized in figures from 53 to 59. Results are only shown for a limited set of data, given that there are not forward or side fall tests with 20 cm feet distance.

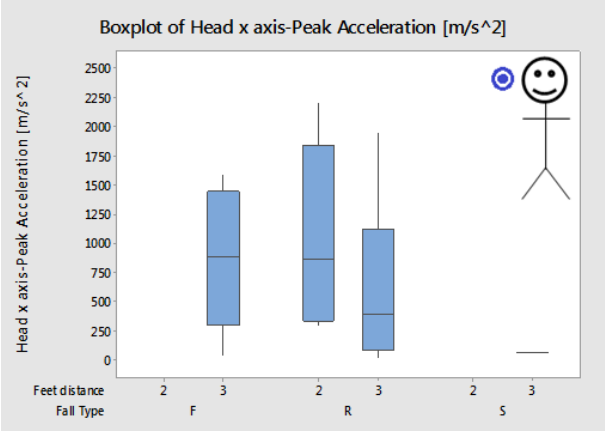

Figure 53 *Peak acceleration boxplot of the head on x axis for varying feet distance condition per type of fall*

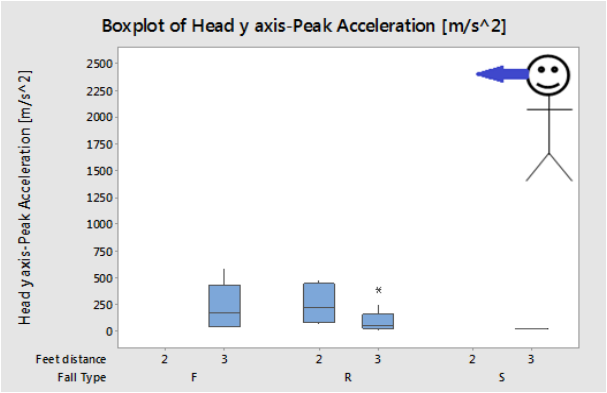

Figure 54 *Peak acceleration boxplot of the head on y axis for varying feet distance condition per type of fall*

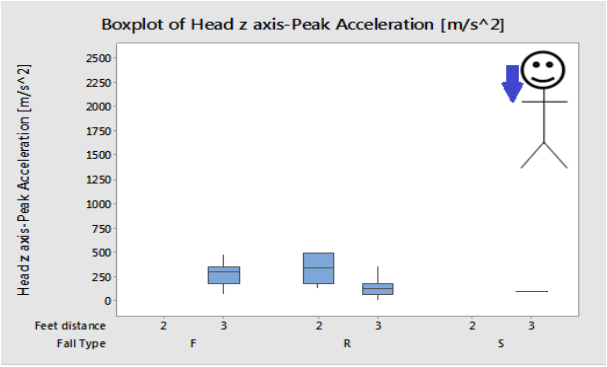

Figure 55 *Peak acceleration boxplot of the head on z axis for varying feet distance condition per type of fall*

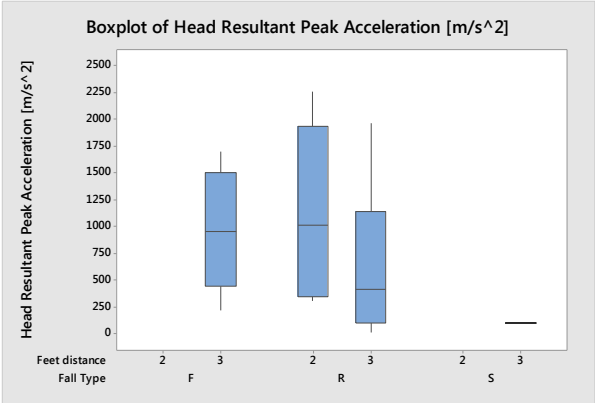

Figure 56 *Peak acceleration boxplot of the head resultant for varying feet distance condition per type of fall*

The peak accelerations on x axis of the head, in rear falls, are larger when the feet distance is 20 cm. Accelerations on the y and z axes are minor, but their magnitude is larger when the feet are 20 cm apart with respect to the situation in which the feet are placed 30 cm apart.

Accelerations at the torso are shown in the next plots

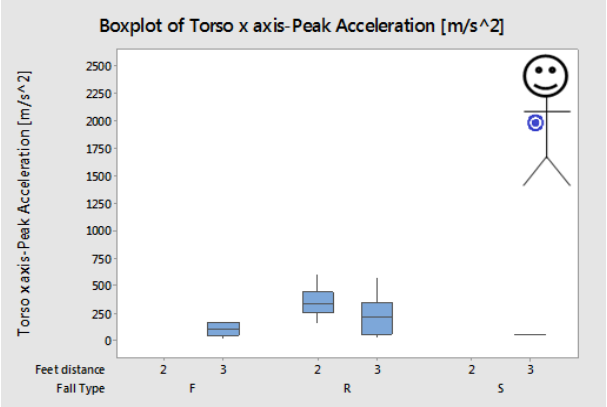

Figure 57 *Peak acceleration boxplot of the torso on x axis for varying feet distance condition per type of fall*

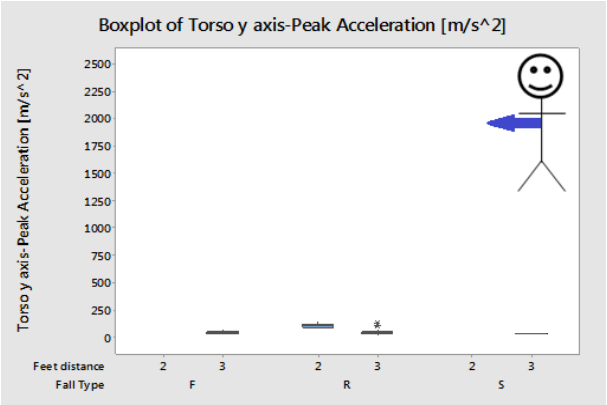

Figure 58 *Peak acceleration boxplot of the torso on y axis for varying feet distance condition per type of fall*

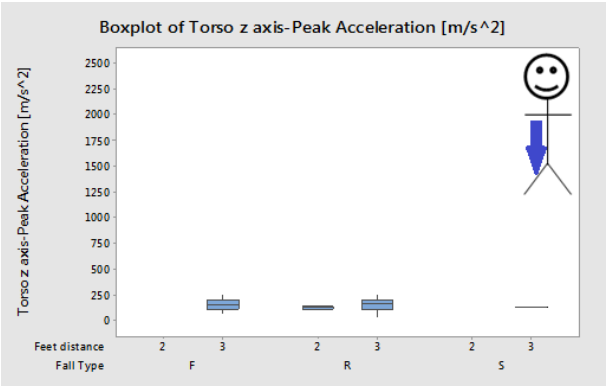

Figure 59 *Peak acceleration boxplot of the torso on z axis for varying feet distance condition per type of fall*

The effect of the feet distance on the acceleration of the torso is similar to what was previously outlined for the head: the acceleration along x axis in rear falls is larger

when the feet are 20 cm apart, y and z accelerations are slightly affected by the feet distance.

3.2 Fall Duration Analysis

Results of the video-based fall duration analysis are summarized in Table 3.

Test ID	Fall Type	Pre fall	Fall Height	Limbs arrest	Feet distance	Obstacles	Fall Duration(s)
1	R	1	8	0A	2	F	1,5
2	R	1	8	0A	2	F	1,4
3	R	1	8	0A	3	F	1,74
4	R	1	8	0A	3	F	1,8
5	R	1	7	0A	3	F	1,57
6	R	1	7	0A	3	F	1,6
7	R	1	6	0A	2	F	1,63
8	R	1	6	0A	2	F	1,2
9	R	1	6	0A	3	F	1,33
10	R	1	6	0A	3	F	1,5
11	R	1	5	0A	2	F	1,47
12	R	1	5	0A	2	F	1,5
13	R	1	5	0A	3	F	No video
14	R	1	5	0A	3	F	1,4
15	R	0	6	0A	3	F	3,9
16	R	0	6	0A	3	F	2,8
17	R	1	7	0A	3	F	No video
18	R	1	7	0A	3	F	2,4
19	R	1	7	0A	3	F	2,1
20	R	1	7	0A	3	F	1,94
21	R	1	5	0A	3	D	1,67
22	R	1	5	0A	3	D	2
23	R	1	6	2A	3	F	2,07
24	R	1	6	2A	3	F	2,47
25	R	1	6	1A	3	F	1,87
26	R	1	6	2A	3	F	1,57
27	F	0	6	0A	3	F	1,57
28	F	0	6	0A	3	F	1,63
29	F	1	8	0A	3	F	1,47
30	F	1	8	0A	3	F	1,33
31	F	1	8	2A	3	F	1,43
32	F	1	8	2A	3	F	1,4
33	S	1	7	0A	3	F	1,43

34	F	1	6	0A	3	D	1,97
35	F	1	6	0A	3	D	1,74
36	F	1	7	0A	3	D	1,9

Table 2 *Nomenclatures and falling durations of the falling tests*

From the table it can be seen that the fall durations of the tests are distributed between 1, 2 and 3, 9 s. The maximum fall duration occurred at Test 15 (R-0-6-0A-3-F) and it is 3,9 second. Test 8 (R-1-6-0A-2-F) has the minimum fall duration which is 1,2 second.

Boxplots are plotted and interpreted in order to understand if the pre-determined factors have distinctive effect on the falling duration and, if they have, how they affect it.

3.2.1 Arm Arrest Effect

By observing the videos, it is expected that if arm arrest is present, the fall time is longer especially for the backward falls (in front falls the arms are close to the chest). Figure 60 confirms the expectations since the duration of two arm-arrested falls are averagely larger and have a comparable variability.

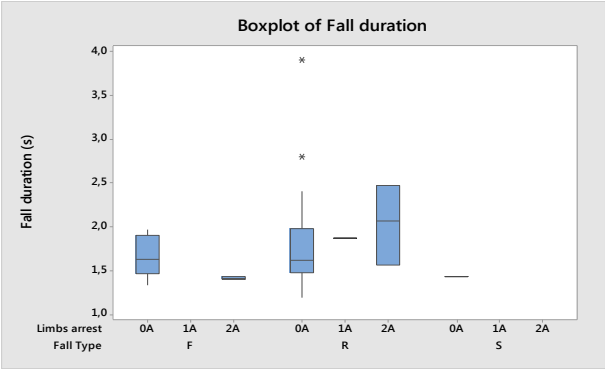

Figure 60 *Boxplot of fall duration for varying feet distance per type of fall*

3.2.2 Fall Height Effect

Fall duration boxplot for varying hips to foot height per type of fall can be seen in the Figure 59. No coherent inference could be made for the effect of varying falling height from the boxplot.

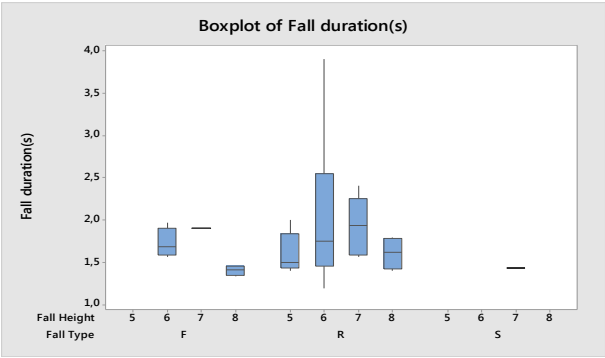

Figure 61 *Boxplot of fall duration for varying falling height per type of fall*

3.2.3 Pre-fall Condition Effect

The effect of the pre-fall posture (sitting or standing) is summarized by Figure 61. Backward falls last are generally longer when the subject is sitting, given that the dummy moves quite slowly after hitting the chair. In front falls, fall durations for the falls from the standing position has a large variability because of the presence of disturbed falls; the medians are comparable. The reason why forward falls from sitting position are longer might be due to the chair presence under the hips of the dummy: the chair prevents immediate downfall just after the quick release of the dummy and the contact of the hips and chair is separated after a certain rotation of the torso. However, in case of free falls, dummy is directly under effect of downward gravitational force just after quick release of the dummy.

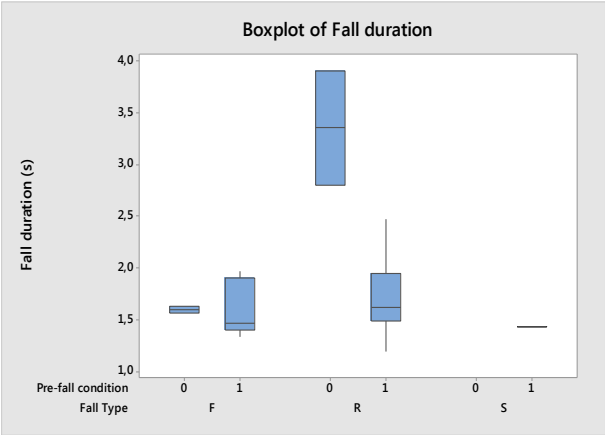

Figure 62 *Boxplot of fall duration for varying pre-fall condition per type of fall*

3.2.4 Fall Trajectory Effect

We can see from the boxplot in the Figure 63 that free falls having disturbed trajectory

have longer fall time with respect to free falls. It is an expected situation because for the free falls, after quick release there are no obstacles to damp the body before it crushes the ground and complete the fall. This damping effect at disturbed falls decreases the accelerations and speeds of almost all parts of the dummy causing longer durations.

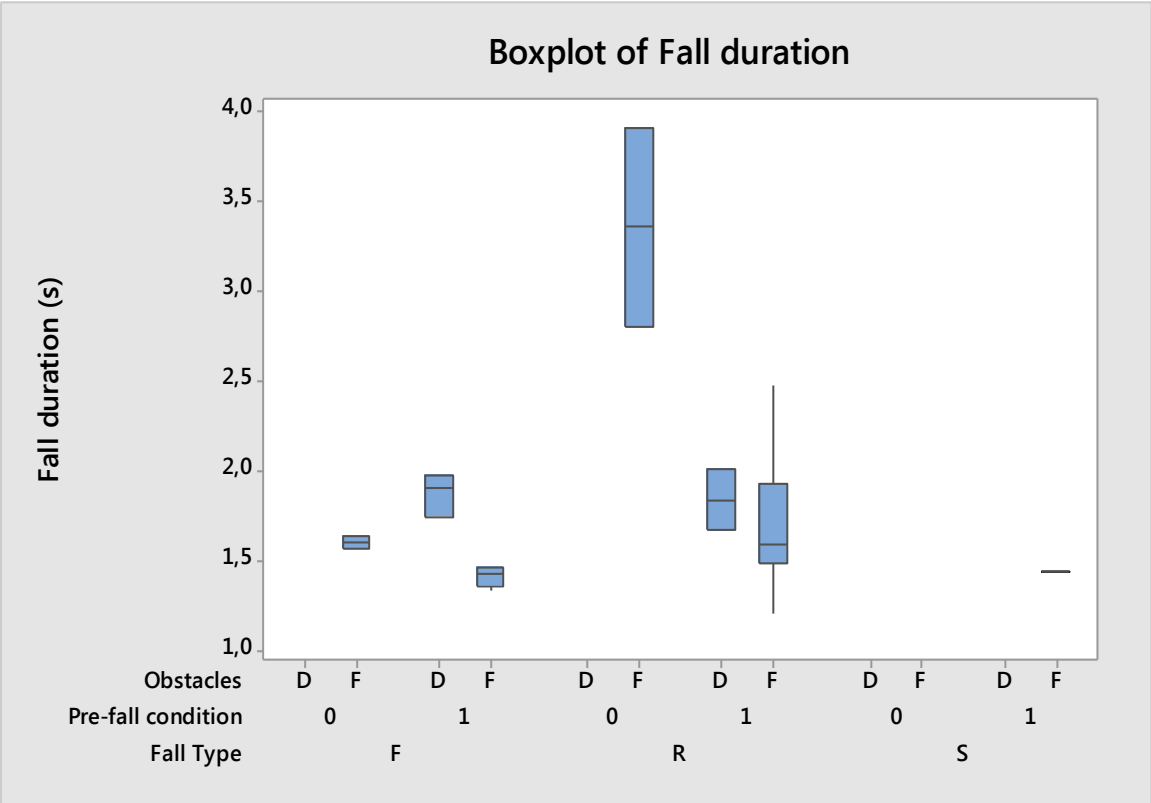

Figure 63 *Boxplot of fall duration for varying pre-fall condition and fall trajectory condition per type of fall*

3.2.5 Feet Distance Effect

The boxplot in the Figure 64 shows that the backward falls having 30 cm feet distance have a longer duration with respect to backward falls having 20 cm feet distance. This might be endorsed to the more stable equilibrium that the dummy has in this position.

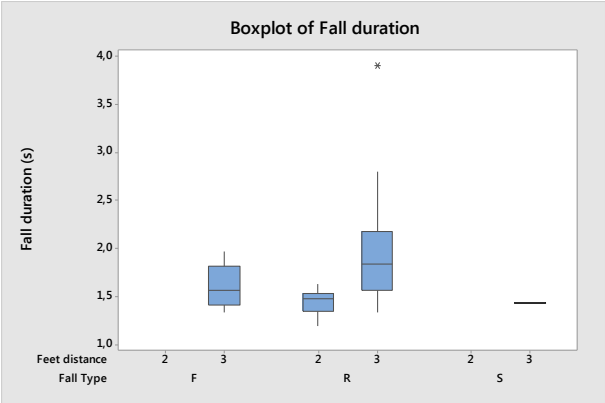

Figure 64 *Boxplot of fall duration for varying feet distance per type of fall*

3.3 Video Processing

First we present here an example of the fall test with ID F-0-6-0A-3-F; the fall configuration and the fall trajectories identified with the image processing described in section 2 are shown in the next two figures.

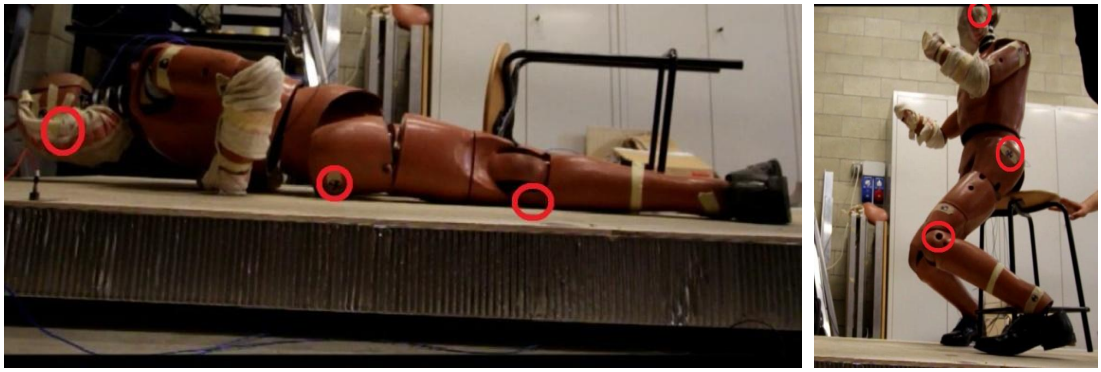

Figure 65 *After fall posture (left), Figure 2. Pre-fall posture (right) with the points marked during analysis of F-0-6-0A-3-F*

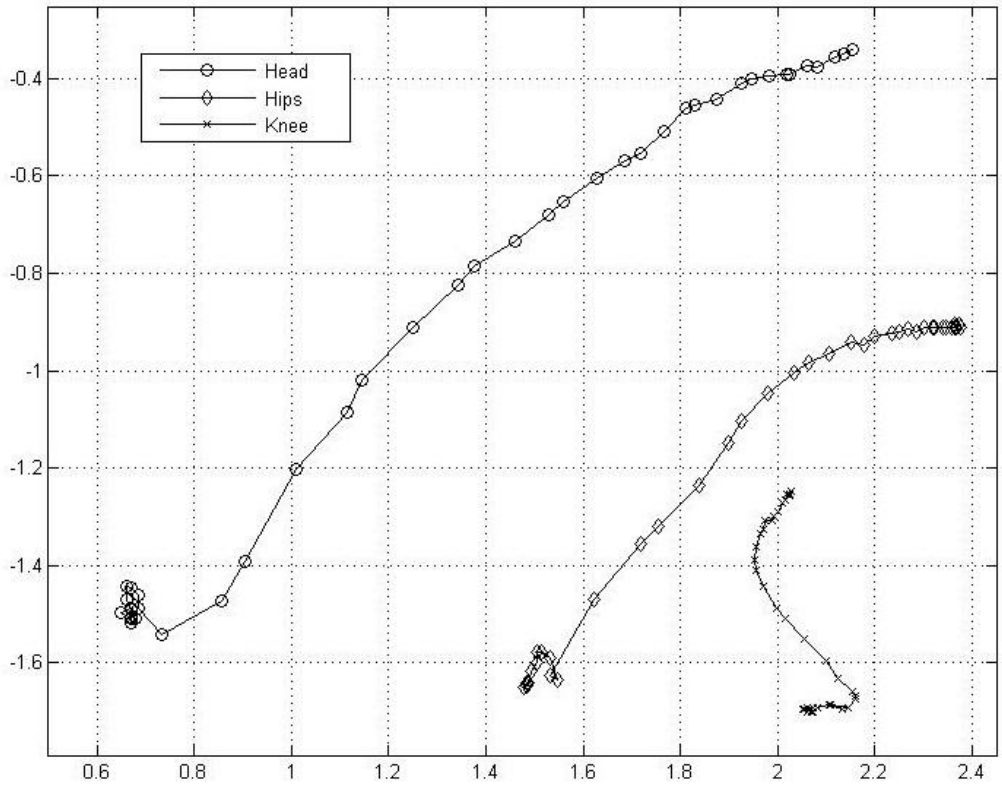

Figure 66 *Trajectories of head, hips and knee for the test F-0-6-0A-3-F*

The trajectories were then used to identify the segments' velocities, which were plotted against the integrated acceleration time history (Figure 67). The acceleration time history was low-pass filtered at 15 Hz and then integrated in time domain. Despite some similar characteristics between the graphs, there are differences that can be endorsed to the manual pattern recognition algorithm adopted.

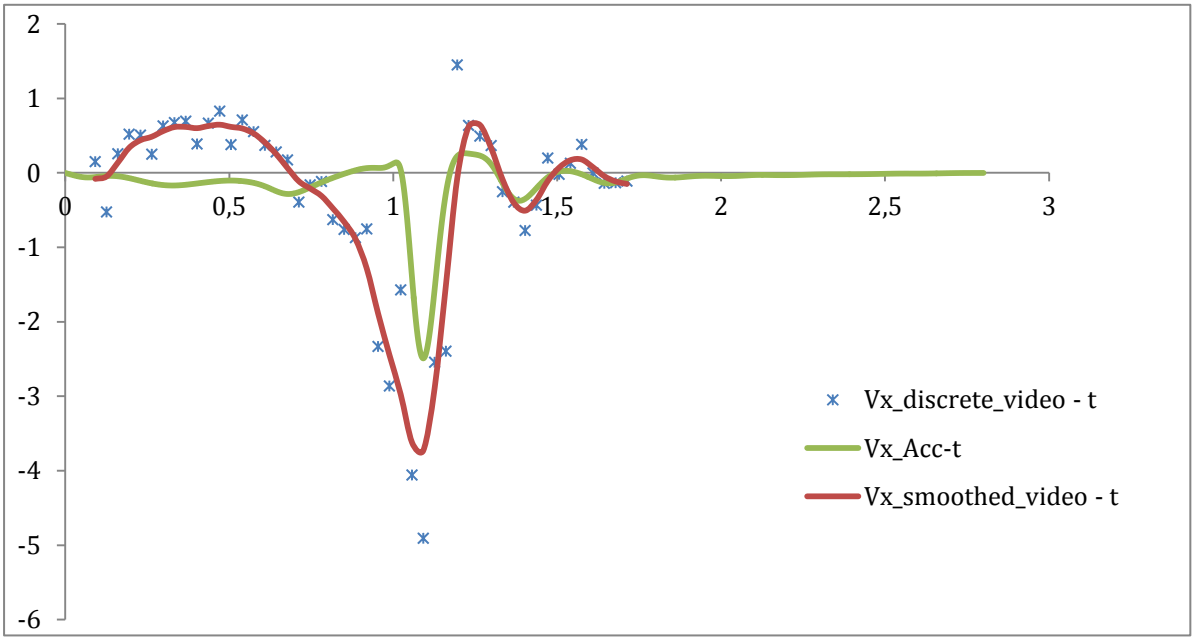

Figure 67 *Velocity comparison (V_{X_HEAD} [m/s] – t [s]) for F-0-6-0A-3-F.*

The next figures show another comparison, the one of test F-0-6-0A-3-F.

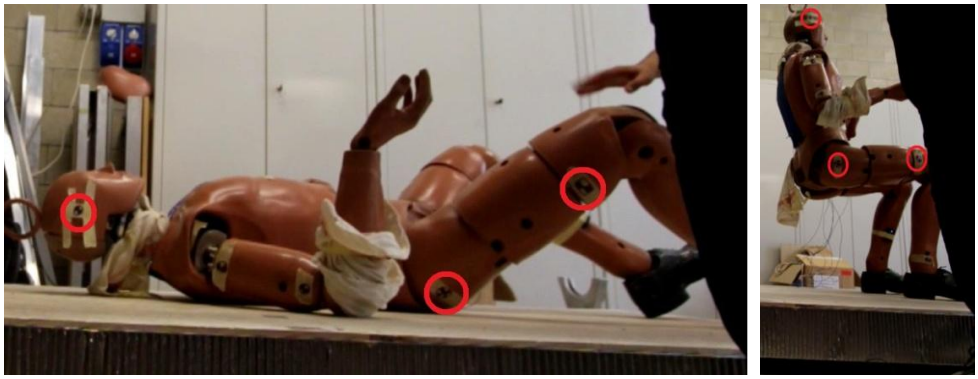

Figure 68 *After fall posture (left), Figure 2. Pre-fall posture (right) with the points marked during analysis of R-1-5-0A-3-F*

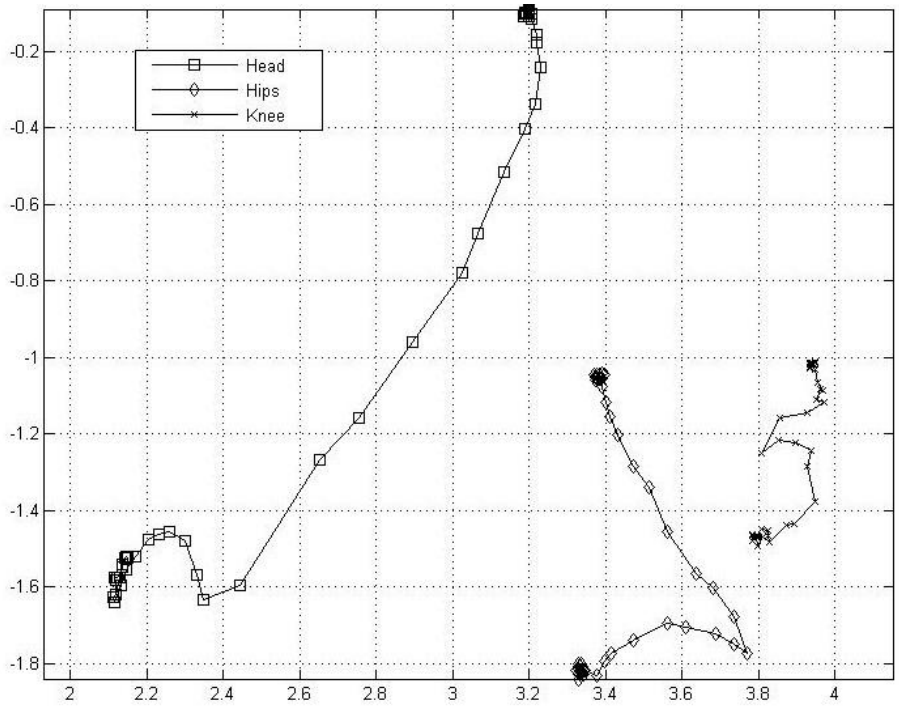

Figure 69 *Trajectories of head, hips and knee for the test R-1-5-0A-3-F*

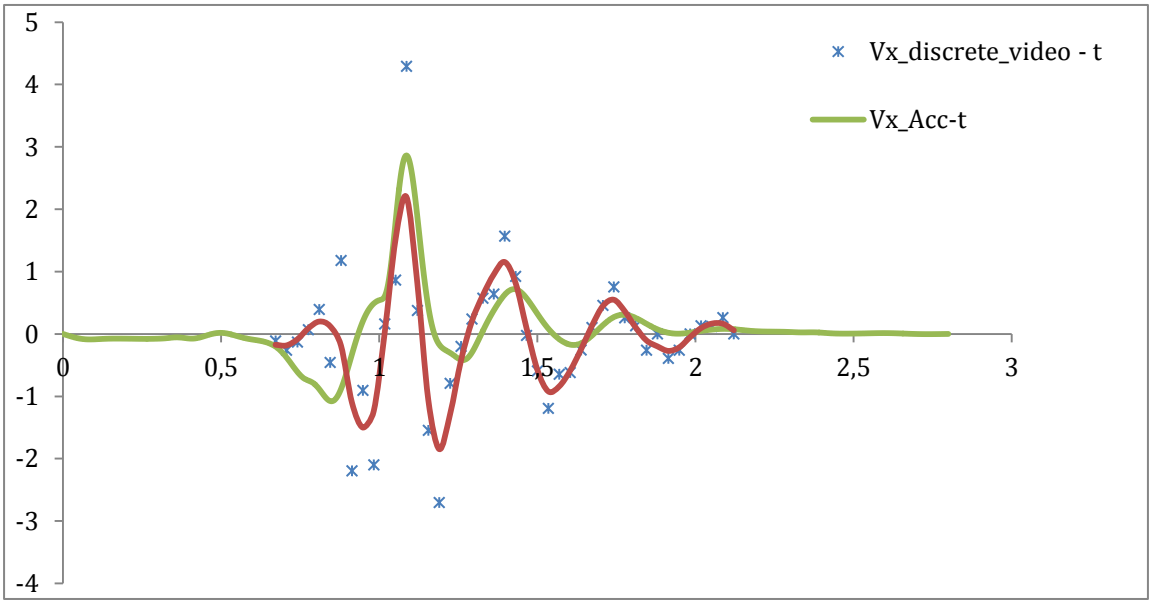

Figure 70 *Velocity comparison (V_{X_HEAD} [m/s] – t [s]) for R-1-5-0A-3-F*

Also for the test R-1-5-0A-3-F, the patterns are similar, although there are noticeable differences in the measured peak amplitudes. Other tests were also processed after the observation of the similarity mentioned above. The processed test videos are belong to free falls since the disturbed trajectory cause the movement of the head inward the plane of the video. So applying this approach is not reliable in this case. Twenty-one videos describing different free falls were processed. For each test, velocity-time plot

obtained by video was compared with the velocity-time plot obtained by integration of the accelerometer. Maximum values of the velocities for the two approaches were compared and errors are summarized in Table 4.

Test ID	Fall Type	Pre-fall condition	Fall Height	Limbs arrest	Feet distance	Obstacles	Maximum Vx_Smoothed from the video	Maximum Vx from the accelerometer data	ERROR
1	R	1	8	0A	2	F	3,35	3,18	0,05
2	R	1	8	0A	2	F	3,16	2,53	0,25
3	R	1	8	0A	3	F	4,31	3,16	0,36
4	R	1	8	0A	3	F	4,12	2,73	0,51
5	R	1	7	0A	3	F	2,36	2,44	0,03
6	R	1	7	0A	3	F	2,42	3,08	0,21
7	R	1	6	0A	2	F	2,00	2,61	0,24
8	R	1	6	0A	2	F	2,06	1,65	0,25
9	R	1	6	0A	3	F	-1,33	-1,05	0,27
10	R	1	6	0A	3	F	2,12	2,43	0,13
11	R	1	5	0A	2	F	3,34	3,49	0,04
12	R	1	5	0A	2	F	4,64	4,15	0,12
14	R	1	5	0A	3	F	2,20	2,86	0,23
18	R	1	7	0A	3	F	2,03	1,77	0,15
19	R	1	7	0A	3	F	1,88	2,07	0,09
20	R	1	7	0A	3	F	1,97	2,13	0,07
28	F	0	6	0A	3	F	-3,58	-2,49	0,44
29	F	1	8	0A	3	F	-3,53	-3,04	0,16
30	F	1	8	0A	3	F	-4,04	-3,42	0,18
31	F	1	8	2A	3	F	-3,57	-3,36	0,06
32	F	1	8	2A	3	F	-3,50	-2,81	0,24
								Max Error	51%

Table 3 *Comparison of maximum velocities found by video processing and accelerometer data, error value for each tests and maximum error*

The maximum error was 51%, while the error and root-mean-square error was 10%

3.3.1 Potentialities of the proposed technique

Finally, two fall videos found on the internet were processed. Some frames of each fall can be seen in the Figure 71 and Figure 73. The falls in these videos are similar to our test falls since they are due to the fainting. The subjects obviously does not have accelerometers attached their clothes; the use of video surveillance camera allows the kinematic analysis of the falls to detect the impact velocity. Velocity-time graphs, found by video processing for rotating x axis of the head, are shown in the Figure 72 and Figure 74.

Figure 71 *Some frames from the forward fall video that is randomly found in the internet for video processing*

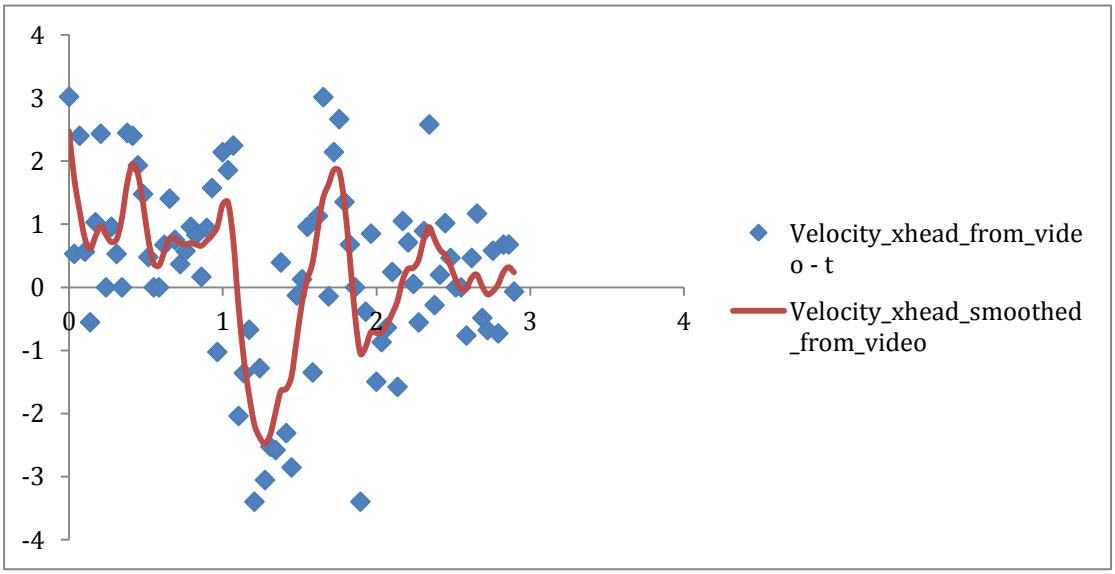

Figure 72 *Velocity of the head of the subject on rotating x axis (V_{X_HEAD} [m/s]) with respect to time (t [s]) for the forward free fall video*

Figure 73 *Some frames from the forward fall video that is randomly found in the internet for video processing*

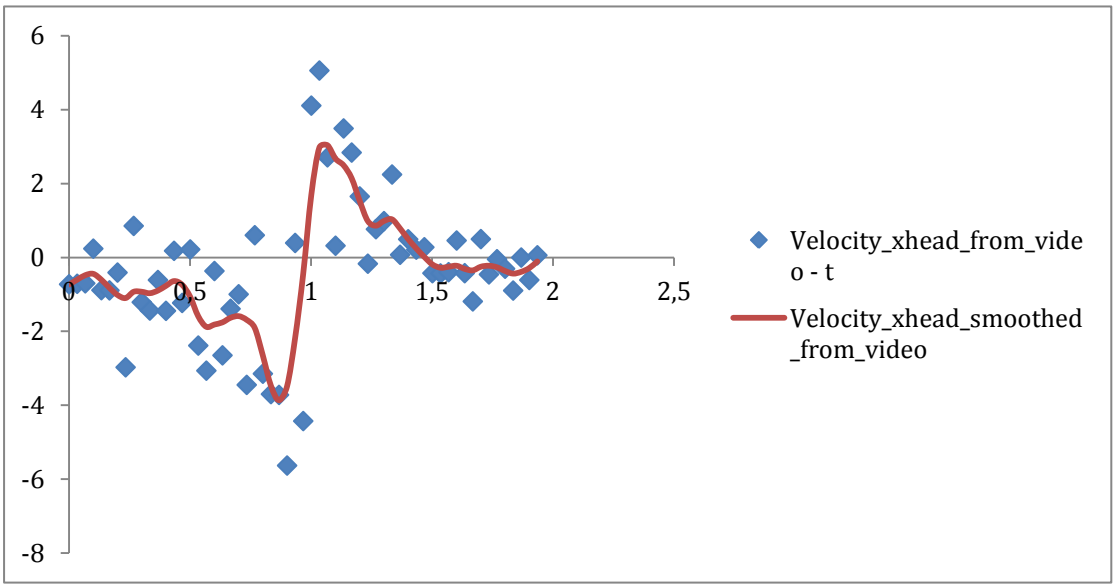

Figure 74 *Velocity of the head of the subject on rotating x axis (V_{X_HEAD} [m/s]) with respect to time (t [s]) for the backward free fall video*

The reliability of these graphs obtained for the videos found in the internet is limited, because of the bad quality of the videos and bad lightening of the environment. The conversion from pixel to real dimension is done by guessing the subjects heights, whose uncertainty is in the range of 10 – 20%. Finally, the subjects are far away from the camera so small marking mistakes have severe effects on the result and the camera is not perpendicular to the subjects. Nevertheless, the peak velocities are comparable to those obtained with our method, pointing out the validity of the experimental results.

4 Discussion

4.1 Peak Acceleration Analysis

Although there are not studies about the influencing factors' effects on the fall, there are number of studies investigating maximum accelerations on the body parts as a result of the falls. It is possible to discuss our work comparing to these studies.

Fanta, Kubový, Lopot, Pánková and Jelen worked on the kinematic analysis of backward falls of subject and dummy. They placed a 3-axial accelerometer in the head of the dummy for the assessment of head injuries. They had done eight tests, three of them were done while a chest impact is applied to the dummy, five of them were performed when a car having 10 m/s velocity hit to the dummy. The dummy were standing position at each test. They measured the resultant acceleration on the head for each test. The results are shown in the Table 5 respectively [7].

	Max. a (g)
Dummy 1	120
Dummy 2	265
Dummy 3	225
Dummy 4	314
Dummy 5	198
Dummy 6	212
Dummy 7	112
Dummy 8	324

Table 4 *Resultant accelerations on the head of the dummy*

The maximum head resultant acceleration values are distributed between 120 g – 324 g interval in this study while our maximum head resultant acceleration values for the backward free falling tests having no arm arrest from standing position are distributed approximately between 13 g - 225 g. The fact that we have lower maximum acceleration range is normal because we simulated falls without any input force and under different pre-postures while they simulated the falls under effect of an input from the same standing posture. So our measurement results can also be used for assessment of head injuries caused by falls of elder people due to unconsciousness.

In another study carried out by A.K. Bourke, J. O'Brien and G.M. Lyons, acceleration

measured from the torso and thigh of the young healthy subjects for the purpose of fall detection. In the study, subjects performed backward, forward and right-left side falls from the standing position with flexible and straight knees. Considering resultant accelerations of torso and thigh, they defined a threshold value for detection of the fall. Our study can be beneficial for detection of this kind of threshold values since number of pre-determined factors are considered not like one factor, knee flexibility, in this case. Falls due to full unconsciousness are simulated better in case of dummy falls. In the study, for the free forward falls performed by subjects, the maximum resultant acceleration on torso distributed from 5.5 g to 11 g. In our study, the acceleration on the torso of the dummy for free forward falls from standing position are relatively higher and distributed from 13 g to 19 g. The difference is most probably due to physical differences between dummy and subjects, the fall breaking instinct of the subjects and diverse testing environments [6].

Peak acceleration analysis was carried out to understand the effect of pre-determined factors on the body parts which accelerometers were placed. So, by placing number of accelerometers to different parts of the dummy might be more beneficial to interpret the fall both kinematic and kinetic point of view. Results that are more reliable could have been reached if we had time to carry out more tests specifically meant to see effects of each pre-determined factor. Since dummy was rented for a short time, we had no chance to do more tests. For the further studies, different pre-determined factors can be defined and examined.

4.2 Fall Duration Analysis

Fall duration analysis was carried out by using visibility advantage of videos to have more reliable time values. The fall duration may be a stable parameter to automatically detect the fall of subjects using wearable devices.

4.3 Video Processing

In the method section of video processing, it is mentioned that the method we followed is manual processing since automatic pattern recognition is not applicable due to blur occurrence caused by high velocities reached by body parts and inadequate lightening. The solution is found by letting the analyser guess and click the tracked pattern or point. However, this is also not a perfect solution because it is very low chance to guess exact spot of the tracked point in case of blur presence. Moreover, the mark that we followed to obtain kinematic information corresponds to a wide area in terms of pixel in the

video so even if we select the marked area at each frame, it does not mean that we are tracking exactly the same point. Also frame rate of the videos are not very high. For these reasons, the trajectories obtained are not continuous and a denoising algorithm has been used to remove noise from the velocity time history.

Camera positioning is another factor that affects the effectiveness of video processing in 2D analyses. In our tests camera is placed well cantered horizontally but vertically it was on the ground due to absence of proper camera stand and inconveniency of the test room. It was rotated to upward to record dummy falling from head to foot. However, this causes a change on the pixel to meter conversion factor along the vertical axis of the video.

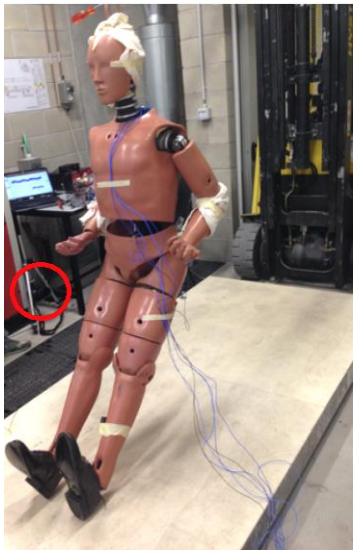

Figure 75 *Camera rotated upward*

Usage of automatic pattern recognition with appropriate positioning of the camera or cameras and with adequate lightening presumably gives trajectories that are more reliable and kinematic information about the body parts of fallen subjects. However, in spite of all these limitations, data were proven compatible with those obtained by accelerometers, enabling the possibility of computing the accelerations from video data; the first attempts in this direction showed that results are generally comparable with those obtained with our dummy.

5 Conclusions

In this thesis, we have analysed several falling tests performed with a dummy in order to simulate the elders' falls. Acceleration have been measured at the head and at the chest along three mutually perpendicular axes. The peak accelerations measured by the accelerometers were compared with the acceleration measured by an image processing system. Accelerometer data was statistically analysed with boxplots, that were used to assess the effect of possibly influencing factors, such as the upper limb posture or the presence of obstacles. Results showed that the most influencing factors are the arm arrest, the presence of obstacles and the distance between the feet, which reduce the peak accelerations at the head and torso. Accelerations measured in falls from sitting position were more severe when falling backwards. The effect of the hips-ground height was not linear. The fall duration (time occurring between the first and the last impact) was performed leveraging on the image processing; phenomena last between 1,2 s and 3,9 s. The sitting pre-posture, the presence of disturbances on the trajectory and the distance between the feet induced a longer fall duration. The effect of fall heights on the duration was not straightforward.

The image analysis was then used to identify the trajectories of the knees, the hips and the head, which were in turn used to derive the joints velocities, afterwards compared to those derived via accelerometer data integration. The velocities identified with the two approaches were compared; the maximum error was 51% and the root mean square of the error was 10%. Results outlined that the image analysis provide for reasonable data even in non-optimal light conditions. This enables the computation of fall parameters from falls movies recorded, for instance, by surveillance cameras.

6 References

[1] Rubenstein, L. and Josephson, K. (2006). Falls and Their Prevention in Elderly People: What Does the Evidence Show?. *Medical Clinics of North America*, 90(5), pp.807-824.

[2] Who.int, (2015). *WHO | Falls*. [online] Available at: http://www.who.int/mediacentre/factsheets/fs344/en/ [Accessed 6 Apr. 2015].

[3] Mubashir, M., Shao, L. and Seed, L. (2013). A survey on fall detection: Principles and approaches. *Neurocomputing*, 100, pp.144-152.

[4] Kerdegari, H., Samsudin, K., Ramli A. R. and Mokaram S. (2012) "Evaluation of fall detection classification approaches, " in Proc. IEEE International Conference Intelligent and Advanced Systems, pp. 131-136.

[5] Jia, N. (2009). Detecting Human Falls with a 3-Axis Digital Accelerometer. *Analog Dialogue, 43*(7), 1-7.

[6] Bourke, A., O'Brien, J., & Lyons, G. (2007). Evaluation of a threshold-based tri-axial accelerometer fall detection algorithm. *Gait & Posture, 26*(2), 194-199.

[7] Fanta, O., Kubový, P., Lopot, F., Pánková, B., & Jelen, K. (2012). Kinematic Analysis of Backward Falls of Pedestrian and Figurine in Relation to Head Injury. *Transactions On Transport Sciences*, *5*(4).

[8] DeGoede, K., & Ashton-Miller, J. (2003). Biomechanical simulations of forward fall arrests: effects of upper extremity arrest strategy, gender and aging-related declines in muscle strength. *Journal Of Biomechanics*, *36*(3), 413-420.

[9] Nihseniorhealth.gov,. (2015). NIHSeniorHealth: Falls and Older Adults - Causes and Risk Factors. [online] Available at: http://nihseniorhealth.gov/falls/causesandriskfactors/01.html. [Accessed 30 March 2015].

[10] Humanetics Innovative Solutions, "Crash Test Dummies," Humanetics, (2015). [Online]. Available: http://www.humaneticsatd.com/crash-test-dummies. [Accessed 10 Apr. 2015].

[11] Ruiz-Shulcloper, J. (2008). *Progress in pattern recognition, image analysis and applications*. Berlin: Springer.

[12] It.mathworks.com,. (2015). Cubic Smoothing Splines - MATLAB & Simulink Example. [online] Available at: http://it.mathworks.com/help/curvefit/examples/cubic-smoothing-splines.html [Accessed 16 June 2015].